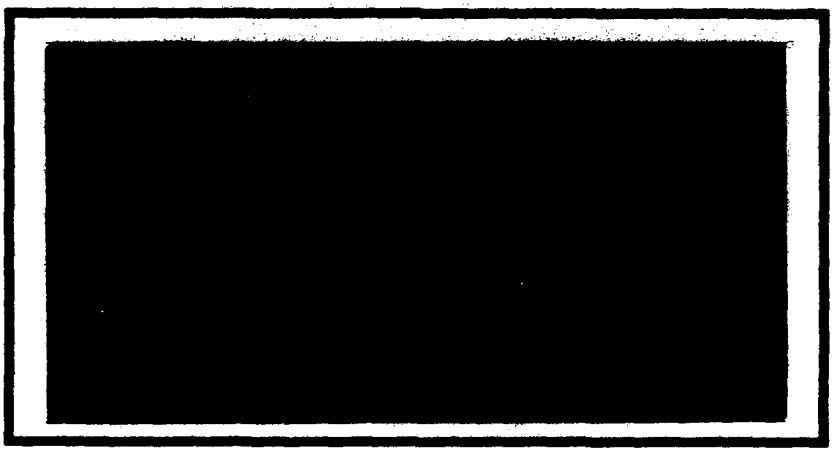

DEPARTMENT OF THE AIR FORCE

AIR UNIVERSITY

AIR FORCE INSTITUTE OF TECHNOLOGY

Wright-Patterson Air Force Base, Ohio

AFIT/GE/ENG/88D-60

A MICROWAVE MEASUREMENT TECHNIQUE FOR COMPLEX CONSTITUTIVE PARAMETERS

THESIS

Michael J. Walker, B.S.E.E.
Second Lieutenant, USAF

AFIT/GE/ENG/88D-60

Approved for public release; distribution unlimited

AFIT/GE/ENG/88D-60

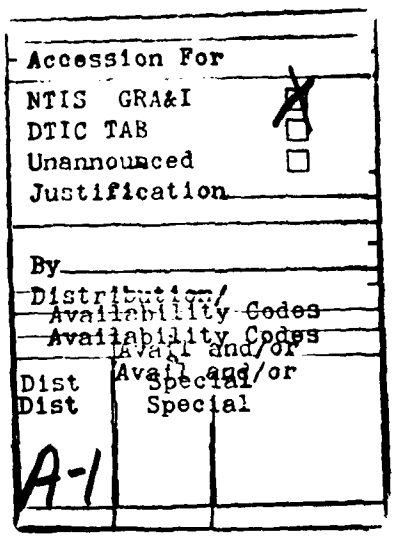

A MICROWAVE MEASUREMENT TECHNIQUE FOR COMPLEX CONSTITUTIVE PARAMETERS

THESIS

Presented to the Faculty of the School of Engineering

of the Air Force Institute of Technology

Air University

In Partial Fulfillment of the

Requirements for the Degree of

Master of Science in Electrical Engineering

Michael J. Walker, B.S.E.E.

Second Lieutenant, USAF

December 1988

Preface

The purpose of this study was to improve a system for measuring the complex constitutive parameters of thin slabs of radiation absorbing materials to include adding the capability to begin examining the inhomogeneity of material. The long term goal of the organization sponsoring this work (AFWAL/AAWP-3) is to develop a fully automated, quality control system which will be able to locate areas of the material in which the parameters deviate to a degree which will cause undesired effects if the material piece is used. Therefore, there was a need to advance the previous capability of making single measurements of marginal accuracy to a more accurate, two-dimensional scanning technique.

I received a great deal of support and assistance in completing this project. I would like to thank my faculty advisor, Major H. Barksdale, for his help and guidance over the last year. I would also like to thank Lt Col Baker for his mathematical assistance, Mr. Ed Utt for his theoretical support, and Mr. Stan Bashore and Mr. Jim Common for their technical assistance. Finally, I would like to thank my wife Judi, who married me in mid-project. Her patience, understanding, and support were the greatest help I could have asked for while I spent most of our first six months together working on this project. She was also responsible for keeping my nose so diligently to the grindstone.

Michael J. Walker

Table of Contents

List of Figures

List of Tables

Abstract

A technique was developed for the measurement of complex constitutive parameters of thin slabs of radiation absorbing material. Parameters include the real and imaginary components of the permittivity and permeability. The conductivity was lumped into a composite imaginary permittivity component through the loss tangent. The homogeneity of the material across the slab's surface and the ability of this technique to locate areas where the parameters deviate from the average was also examined.

The transmission coefficients of the slabs were measured at several angles of incidence using a 180 degree, bistatic configuration. This permitted a computer program to solve the nonlinear system of transmission equations for the desired parameter values. The technique and computer program are applicable to measurements taken at either perpendicular or parallel polarization, and takes advantage of prior known material qualities, nonmagnetic or lossless, to reduce the order of the system. Measurements were taken at 94 GHz using a Gunn phase-locked oscillator as a source. A pair of conical horn-lens antennas and a Scientific Atlanta 1783 Programmable microwave receiver were the primary pieces of equipment required.

Tests and measurements showed this system was an improvement over previous capabilities. Pseudo-parameter variations of ten percent or more, produced by physical alteration of specific regions of the material, were detected in the parameter outputs even when they were not detectable in the measurement values alone.

A MICROWAVE MEASUREMENT TECHNIQUE FOR COMPLEX CONSTITUTIVE PARAMETERS

I. Introduction

Background

The interactions of any object with electromagnetic energy are determined by the object's constitutive parameters; its permittivity, permeability and conductivity. To know the parameters of an object allows the knowledge, through calculation, of any of these interactions. Therefore, it is of great interest to develop accurate techniques for measuring these parameters.

The constitutive parameters of a thin slab of material are often determined by measuring the scattering parameters of a piece of the material cut to the cross section of a waveguide, and then calculating the unknown parameters. Because these parameters are frequency dependent, as the frequency range increases, the size of the waveguide decreases. The complexity of the material's structure often limits the smallest sample size which can fit into the waveguide and still be accurately measured. This sets an upper limit on the frequency. This technique also includes the assumption that the sample being measured in the waveguide has the same parameter values as the entire piece; that the slab is homogeneous.

The present need for material parameter information goes beyond these limitations. The range of frequencies being used today includes increasingly higher values, and the production of more complex materials, such as metallic and fiber loaded composites and ceramics, and layered materials, leads to more anisotropic characteristics. Therefore, a different technique for determining the material's parameters is required.

Previous work has shown that the parameters of a slab of material mounted in free-space can be determined from transmission and reflection measurements. This switched the limitation on the measurement frequency from being determined by the material to being determined by the upper limit of the equipment. However, the assumption of homogeneity was retained in each case, and most efforts determined only the real component of the permittivity, assuming the others to be known.

Overview

This technique determines both the real and imaginary components of the permittivity and permeability. It also examines the material's inhomogeneity in an effort to locate "hot spots", areas where the local constitutive parameter values are in great contrast to the average parameter values. To do this, the complex parameters of a slab are determined at an array of discrete points across the slab's surface to examine their two dimensional variance. The bulk parameter values determined are constants in the third direction, through the thickness of the

slab, although the material may actually be layered with different parameters from layer to layer. The parameters are assumed constant in a small region around each measurement point because the incident radiation has a finite beamwidth. Although the material is no longer treated as completely homogeneous, it must still be treated as locally homogeneous to allow a workable level of discretization.

Scope

This work is only meant to be a preliminary technique and proof of concept for the analysis of the two dimensional inhomogeneity of a sheet of material. The inhomogeneity of the material will not be determined continuously across the sheet, but only in discrete steps. Due to the current limitations of the equipment available, all work and measurements are done at a single frequency, although the technique is applicable to any frequency. In fact, extending this concept to a broad range of frequencies would allow diagnostic imaging of a planar sample to locate the position and depth of "hot spots" within the sample. The parameters are indeterminable near the edges of the material to avoid the problems associated with making measurements in that region. This technique is flexible enough to allow perpendicular or parallel polarization measurements to be used. It also takes advantage of any previously known parameter values or material qualities, if they are available.

Preview

The next chapter is a literature review. It describes the previous work in parameter measurement and their contributions to this technique, and sets the stage for chapter three which describes the analysis incorporated by this technique. Specifically, chapter three develops the information supplied by the literature review into a workable system and describes how the measurements are made and how they are processed into the final product, the parameters. The fourth chapter will review the results obtained by application of this technique to both tests and real situations. The final chapter will conclude with a summary of the technique and results. It will also supply recommendations for further development and effort in this area. All of the referenced computer programs used by this technique will be supplied in the Appendices.

II. Literature Review

Inverse Problems

Electromagnetic inverse problems are attempts to derive unknown information about an object from its measurable effects on known incident electromagnetic radiation. Research efforts involving inverse problems range from theoretical to practical, and have already resulted in many technological applications. In a special issue of IEEE Transactions on Antennas and Propagation dedicated to electromagnetic inverse problems the topics were categorized into six areas allowing 576 possible combinations for different studies (4:188).

Mathematically, inverse problems are difficult to solve. In most cases, simplifying assumptions need to be applied to the problem to achieve an answer. Because each research effort has the possibility of making different assumptions, there are literally thousands of possible research areas in the field of inverse electromagnetics.

This research falls under the category of constitutive parameter determination; calculating the permittivity, permeability, and/or conductivity from scattering measurements. This is still a very broad area of interest. Research has varied in the choice of the parameters of interest, the shape of the object under test, the measurement technique and equipment, and the final calculation method, as well as the approximations and assumptions in each of these areas.

Parameter Choice

The choice of which parameters are to be determined is the first differentiator of constitutive parameter identification work. There are five possible parameters of interest; the real and imaginary components of both the permittivity and permeability, and the conductivity. Other parameters, such as the loss tangent, wave number, or index of refraction, are functions of these five. The choice is not so much which parameters need to be determined, but which ones do not. After assuming the material possesses certain qualities which define some of the parameters as known constants, or otherwise assuming a parameter profile to be known, the parameters to be determined are those which remain unknown. Assuming a material is lossless requires that the conductivity and the imaginary components of both the permeability and permittivity are zero. The assumption of a nonmagnetic material sets the permeability equal to that of free space.

The loss tangent affects a material's scattering qualities in the same way as the imaginary component of the permittivity and is a function of the material's conductivity. The imaginary component of the permittivity can be assumed to be zero and its effects attributed to the conductivity through the loss tangent, thereby reducing these three unknown parameters to two. In another method of reducing these parameters, the loss tangent and the imaginary permittivity component can be lumped into a composite imaginary part of the permittivity.

Once it has been determined which parameters are to be calculated, another assumption to be made is whether or not the material is homogeneous and, if not, to what degree. To simplify analyses and calculations, inhomogeneous parameters have been assumed in some cases to be a function of the variable in the direction of propagation (3:660), or a radial variable out from the object's center in others (12:232). Another method is to model the inhomogeneity by assuming the object to be locally homogeneous; to assume the parameters are constant within regions but different from one region to the next.

This measurement technique determines all four parameters in the complex permittivity and permeability. It incorporates the conductivity into a composite imaginary component of the permittivity. It also assumes these parameter values are constant in regions around each measurement point, but vary from point to point. The following equations define the relative permittivity and permeability used (10:15-18).

$$\mu_r = \mu' - j\,\mu'' \tag{1}$$

$$\epsilon_r = \epsilon' - j\,\epsilon''_c \tag{2}$$

$$\epsilon''_c = \epsilon'' + \sigma / \omega \tag{3}$$

From this point forward, the subscript 'c' will be dropped, and any occurrence of ϵ'' will actually be in reference to ϵ''_c.

Material Shape Choice

The next consideration in the inverse problem of determining constitutive parameters is the choice of the shape of the object whose parameters are of interest. When using free space measurement techniques, the shape of the test objects can be one of a great number of varieties, however spheres, cylinders, and planes predominate. Spheres are simplest and have been used directly as well as for the shape of regions of discrete, lossy scattering within an otherwise homogeneous material (5:371). Cylinders are usually oriented with their axis perpendicular to the direction of propagation, and can be varied in many ways. They are a convenient shape for two dimensional analysis when inhomogeneous parameters are assumed a function of a radial variable from the objects center as illustrated in Fig. 1 (12:232). They have also been treated as a series of locally homogeneous, concentric cylinders of specified thickness, each with constant parameter values within its region, see Fig. 2 (2:1573; 8:392). Although no cylinder can truly be infinitely long, it is another useful analytical assumption because it makes the analysis of the measured data theoretically simpler. This assumption can be made when the interactive effects of the edges of the cylinder ends can be assumed negligible (7:364; 11:1448; 12:232).

In the category of planar objects, the choice tends to stay within two broad subcategories. The first is that of a half-space, extending to infinity in both directions in two

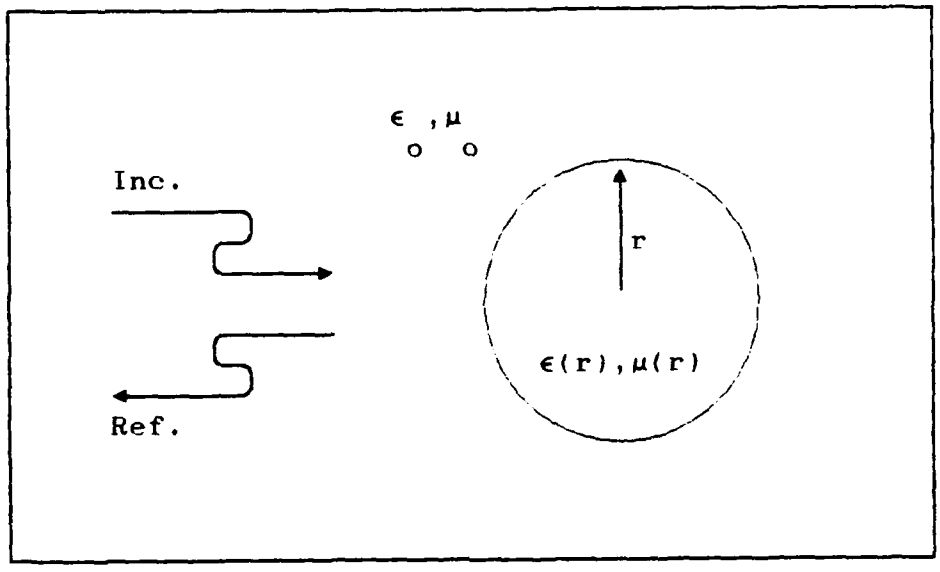

FIGURE 1. Cylindrical Model, Radial Parameters

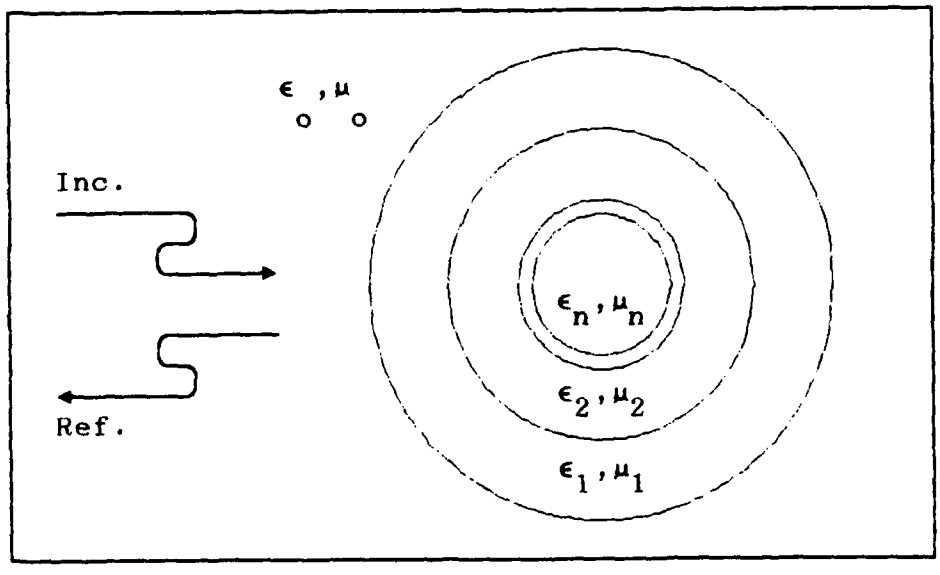

FIGURE 2. Layered Cylinder Model

rectangular coordinates while beginning at a specific point and extending to infinity in only one direction in the third, as in Figure 3. The second is a layer, extending to infinity in both directions in two rectangular coordinates, but with a finite thickness in the third, shown in Figure 4. Again, infinite sized objects are not physically realizable, but are analytically simpler and can be approximated reasonably well (3:658; 5:372; 13:660; 14:1409). Planar objects can also be varied by dividing a single layer or half-space into a finite or infinite number of consecutive locally homogeneous layers, see Figure 5.

Other than these three primary shapes, there are a few other choices which have been used. The object has been modeled in some cases as a homogeneous medium of known constant parameter values, but with a distribution of discrete scatterers with unknown parameters within it, as mentioned above with relation to spherical shapes (5:371). In this case, the distribution method applied to the scatterers can be varied. Another model chosen

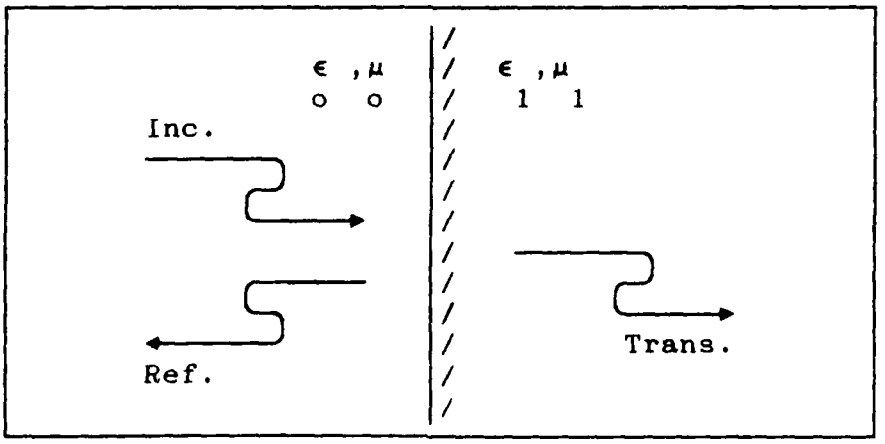

FIGURE 3. Semi-Infinite Planar Object Shape

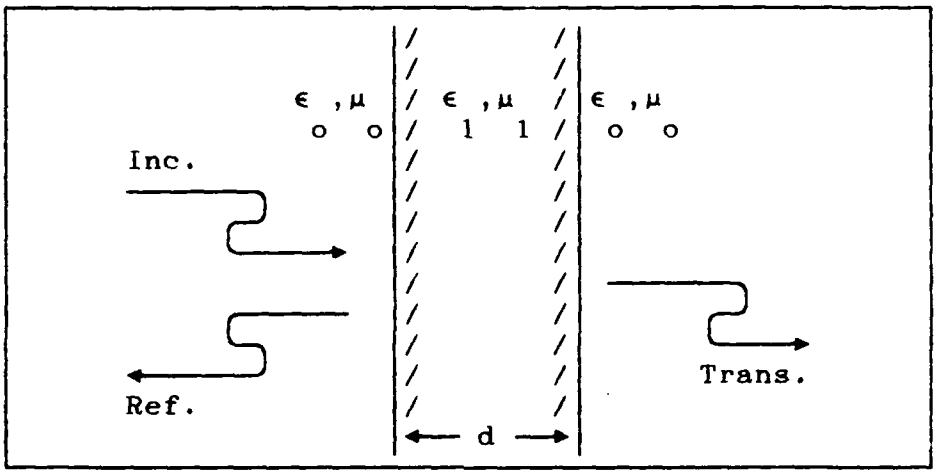

FIGURE 4. Finite Planar Object Shape

for parameter measurement work is a plasma because of its applications to atmospheric electromagnetics.

This measurement technique works with a planar slab of material of finite thickness. For analytical simplification, the parameters are modeled and calculated as if they were constant through the thickness of the material, even if the material is actually layered.

Measurement Technique

The next major difference in parameter measurements are the choices of measurement technique, equipment, and positioning. The free-space technique has already been mentioned, but the parameters can also be determined from scattering measurements of a waveguide system containing a section of the material. This technique limits the object choice to being a planar shape. It also limits the frequency of measurement, as the structure or

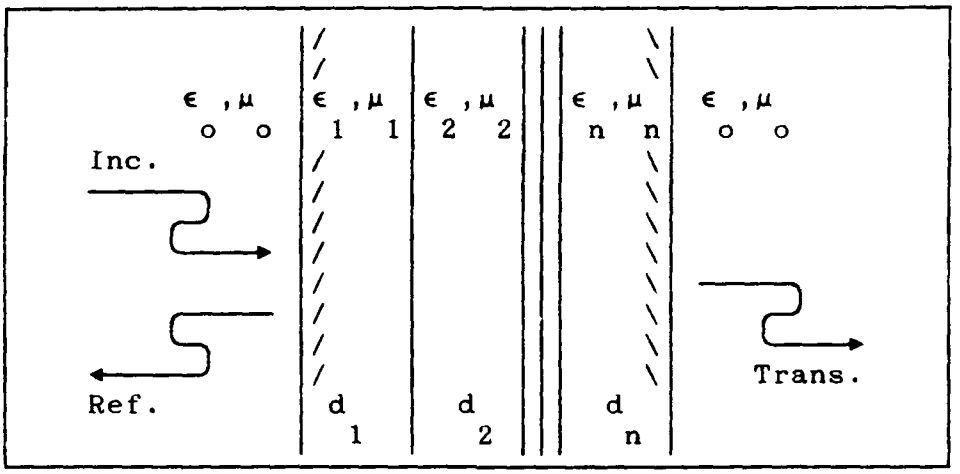

FIGURE 5. Finite Multi-Planar Object Shape

strength of some materials will not allow a sample size small enough to properly fit in a waveguide at higher frequencies.

Using the free-space technique also allows greater flexibility. The equipment can be employed in a monostatic configuration, in which the source and receiver are the same device. This situation requires the source to be pulsed to separate the incoming and outgoing signals. The equipment can also be in a bistatic configuration with the source fixed and the receiver either aligned opposite the object under test or at variable angles and a known radial distance. When the object is planar, the measurements can be done at either normal or variable incidence angles. If both the source and receiver are fixed, and measurements at several angles are required, the object must be rotated (10:45). The devices can also be positioned so that the object is in the Fresnel or near field regions (16:342), although most measurement work has been done in the far field.

Another technique choice concerns the actual type of measurements to be made. The reflected radiation, the transmitted radiation, or both can be measured and used to determine the parameters, and measurements of either the magnitude or phase, or both, can be made in each case. In the work of Shimabukuro, Lazar, Chernick and Dyson, the magnitudes of both the reflected and transmitted waves were measured, and it was found that the reflected waves caused some errors in measurement at angles close to normal due to multiple reflections (13:662). For this reason, Joseph chose to measure only the magnitude of the transmitted wave for better accuracy, but this required a repetition at four different angles of incidence in order to determine the four parameter values (10:34).

The choice of polarization also becomes important when taking measurements in this fashion because the reflection and transmission coefficients are different for each. When the angle of incidence is also being varied, the reflection coefficient has the potential of being zero if the incident wave is at the Brewster angle.

This measurement technique incorporates a free-space, bistatic measurement configuration, with the bistatic angle fixed at 180 degrees. The magnitude of the transmission coefficient is the only measured value. To solve for the four parameters, measurements are taken at four angles of incidence, thus requiring the material be mounted in a support which rotates. Because the parameters are assumed only locally homogeneous and

must be determined at multiple points on the materials surface, the support must also allow the center of each measurement point to be aligned with both the transmission axis and rotation axis.

Data Analysis

The final area in which parameter determination work varies is that of the choice of method by which the parameters are calculated from the measurements. One method is to perform a space-time discretization of the integral equations for the scattered fields, and then solve them numerically (3:658; 15:239). Another method that has been used is to apply the Born approximation to the integral equation to convert it to a solvable form (1:1011; 2:1567).

In many cases, the parameters are determined from the nonlinear system of the equations for the measured values. In the perturbation method, the parameter values of interest are set equal to a constant, or known variable, plus a small unknown variable. Weston used this change of variables in his nonlinear transmission and reflection coefficient equations, then expanded them and kept only the predominant linear pieces. Doing this, he approximated his nonlinear system of equations by a solvable linear system (17:755). Another nonlinear system technique is to use a conjugate gradient method to solve for the scattering matrix (11:1453).

There are also a number of iterative techniques. These methods start with an initial set of guessed solutions, and

compare calculations of what the measurements would have been for these values with what the measurements actually were to determine the changes necessary to remove the error between the two. The final values are determined by repeating this until a certain accuracy level or a repetition number has been achieved. Shimabukuro, Lazar, Chernick and Dyson applied a least squares estimate and resampling technique to iteratively solve their nonlinear system of equations (13:663). Similarly, Joseph used an iterative steepest descent technique to solve his nonlinear system of equations (10:26).

A system of four nonlinear transmission coefficient equations results from the measurement technique as chosen so far. They are processed using an iterative computer program using an updated version of Joseph's steepest descent method in combination with the Newton method. If the variation of the parameters from one measurement point to the next is assumed small, the steepest descent solution for one point can be used as the starting point for the Newton method at all of the measurement points; this results in a saving of computer processing time. Both of these methods will be reviewed further in the next chapter.

Conclusion

This has been an outline of the many ways that work is being done in the area of constitutive parameter measurement. It has also outlined all of the choices made for measurements by this

parameter determination technique. These choices establish a material measurement system which was analyzed to allow the material's constitutive parameters to be calculated from the measurements taken. This analysis is the subject of the next chapter.

III. Analysis

Introduction

In the previous chapter all of the necessary choices and assumptions were made to allow development of a constitutive parameter determination technique. The complex permittivity and permeability of a slab of material with a finite thickness were chosen to be determined, and the parameters were also assumed to be locally homogeneous in the two dimensions across the slab's surface, and constant in the third dimension, its thickness. A free-space, 180 degree constant bistatic configuration for the measurement of the magnitude of the transmission coefficient, at four angles of incidence was also chosen.

Equations

These choices allow the same equations Joseph developed for the transmission coefficient and his steepest descent algorithm computer programs to be used. The equations were checked for accuracy using his equivalent circuit technique, and double-checked using a second-order boundary value technique; from this point forward they will be treated as correct. The equations for the transmission coefficient are on the next page (10:28).

To calculate the magnitude of the transmission coefficient, Joseph multiplied T by its complex conjugate, which actually gave him $|T|^2$. His equations for $|T|^2$ and its partial derivatives with respect to each parameter were all calculated using pure

algebraic techniques, and were very long and complicated. Fortran can calculate the magnitude of T using the intrinsic complex functions CABS or CONJG. Therefore, the computer programs used in this technique will not use Joseph's expanded equations to calculate $|T|$, but will use simplified versions of them and will include the use of complex calculations wherever it is possible and advantageous.

$$T = 1/\{\ \cos(\delta) + j(Z + 1/Z)\sin(\delta)/2\ \} \tag{4}$$

where

$$I = (\mu_r \epsilon_r - \sin^2(\theta)) \tag{5}$$

$$\delta = 2\pi(d/\lambda)I \tag{6}$$

$$Z = \begin{cases} \mu_r \cos(\theta)/I & \text{(perpendicular polarization)} \quad (7) \\ I/\epsilon_r \cos(\theta) & \text{(parallel polarization)} \quad (8) \end{cases}$$

d = slab thickness

θ = angle of incidence

λ = wavelength

Computer Programs

The steepest descent algorithm which Joseph used to obtain his parameters from his measured values was presented step-by-step in Numerical Analysis by Burden and Faires. It uses the gradient, a vector derived from the partial derivatives of the transmission coefficient magnitude, to iteratively adjust the initial parameter guesses in the direction which will cause the

transmission coefficients for these guessed values to approach the measured input transmission coefficient values. It has the advantage of global convergence (6:511), yet it is slower and less accurate than some of the other possible methods.

This program was upgraded by simplifying the equations, but leaving the basic structure of the program alone, as Burden and Faires suggest, to provide a sufficiently accurate initial approximation for a faster, more accurate technique. It also includes a second solution loop written from a Burden and Faires algorithm for the Newton method of solving simultaneous nonlinear equations (6:499). The Newton method is also an iterative method. Instead of the gradient, however, it uses the Jacobian Matrix, a matrix of partial derivatives, to correct each set of guessed parameter values towards a solution set whose transmission coefficients most accurately match the measured values, which does not ensure global convergence. The Newton method programming uses a subroutine which performs Gaussian elimination with partial pivoting to solve the matrix equation for the parameter corrections (9:29-30).

The steepest descent method calculates the transmission coefficients at each angle at least four times per iteration, changing the guessed parameter values slightly each time. Then, it compares the results of each guessed parameter set, and chooses the set whose transmission coefficient magnitudes most closely match the measured magnitudes as the initial parameter set for the next iteration. The Newton method requires most of

the same calculations, including the transmission coefficient and four partial derivatives for each of the four measurement angles, but only calculates them once per iteration. Thus, an advantage of the Newton method, in comparison to the steepest descent method, is that it is faster, providing quadratic convergence (6:498). However, it can diverge if the initial parameter guesses are not accurate enough. This is why the two techniques are used together. All of these equations are derived in Appendix A, and the program is listed and reviewed in Appendix B.

Experimental Setup

The setup for the measurement of the transmission coefficients has already been briefly described as a bistatic configuration with a constant bistatic angle of 180 degrees. The material slab was mounted between the two antennas, and the measurement and parameter calculation process was repeated at an array of points across the material's surface. It has also been mentioned that the mount for the material must allow for rotation of the incidence angle and translation of each measurement point to the rotation and transmission axis. But this only describes a few important points about the experimental setup.

The organization which sponsored this work, AFWAL/AAWP-3, provided the source and receiver equipment for transmission, reception, and measurement at 56 and 94 GHz. To determine the spacing between measurement points, the size of the local homogeneities, it was intended that the centers of each area be

far enough apart that any energy transmitted through surrounding areas would be negligible compared to the energy transmitted through the area of interest. The average sample size was predicted to be one foot on each side.

The distance between the centers of adjacent measurement regions must be dependent on the antennas' beamwidth and the spacing between the antennas and the material. Originally, it was expected that the beamwidth would be the angular width of the antennas' radiation pattern at an arbitrarily chosen decibel level. But the antennas being used have dielectric lenses which change the aperture field to a planar wave. Therefore, it was not necessary to be at the usual far-field distances because a spherical wave pattern did not need to expand until a small central portion could be assumed planar. Instead, the near-field was preferable to take advantage of the planar quality of the fields before they become distorted. At these distances, there was also much less need for the usual far-field configuration's protection from side lobe reflections off of the surrounding walls, floor, and ceiling. But, there are also disadvantages at these distances due to the proximity effects of the antennas.

The determination of the distance between the antennas and the material sample was now a matter concerning multiple reflections between the antennas themselves. It was desirable to locate the antennas close to the material to minimize the distortion of the planar quality of the fields. But at these distances, a standing wave could be established between the

antennas due to superposition at the receiving antenna of the primary radiated field and the first component which was doubly reflected; first off of the receiving and second off of the transmitting antennas, as shown in Figure 6. The substitution of different samples between the antennas would establish different standing waves in comparison to each other and to the reference case, which had no material sample.

Therefore, the separation distance of the antennas had to be great enough that the doubly reflected component was sufficiently attenuated. This can be determined by measuring the received power, when no sample is present, at increasing distances until the fluctuation of the standing wave is sufficiently reduced. In the situations when a sample is present, the attenuation of the doubly reflected component will be even greater as it must pass through the material three times. The angles of incidence must also be kept away from zero to prevent the component which is reflected off both the receiving antenna and the material sample from establishing similar standing waves, since it has only been attenuated by the material once and has propagated a shorter

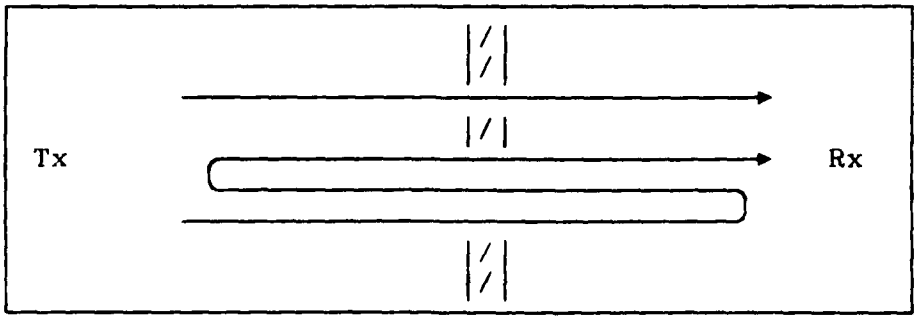

FIGURE 6. Primary Standing Wave Components

distance, see Figure 7. The separation distance will be established through experimentation in the fourth chapter.

Returning to the spacing between measurement areas, the beamwidth could not be any smaller than the three inches of the antenna's diameter in this near-field region, and would have spread very little. Therefore, three inches was assumed to be the beamwidth at this point and it was used to establish the spacing. However, the spacing must actually be the distance between regional centers which, at the maximum angle of incidence, has a perpendicular component equal to the beamwidth. In the material sample a foot square in size, a three inch spacing would provide a 4 by 4 array of measurement points but would allow for no rotation without the beamwidth overlapping into other areas. Scaling down to a 3 by 3 array, with four inches between centers, a rotation of 40 degrees could be made without any beamwidth overlap, as shown in Figure 8. Therefore, a spacing system of four inches center to center was chosen, with a maximum rotation angle of 40 degrees to achieve a nine point measurement system within a foot square sample.

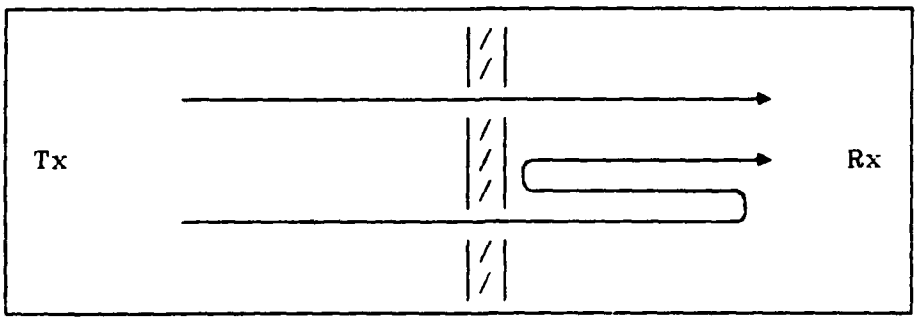

FIGURE 7. Near Normal Standing Wave Components

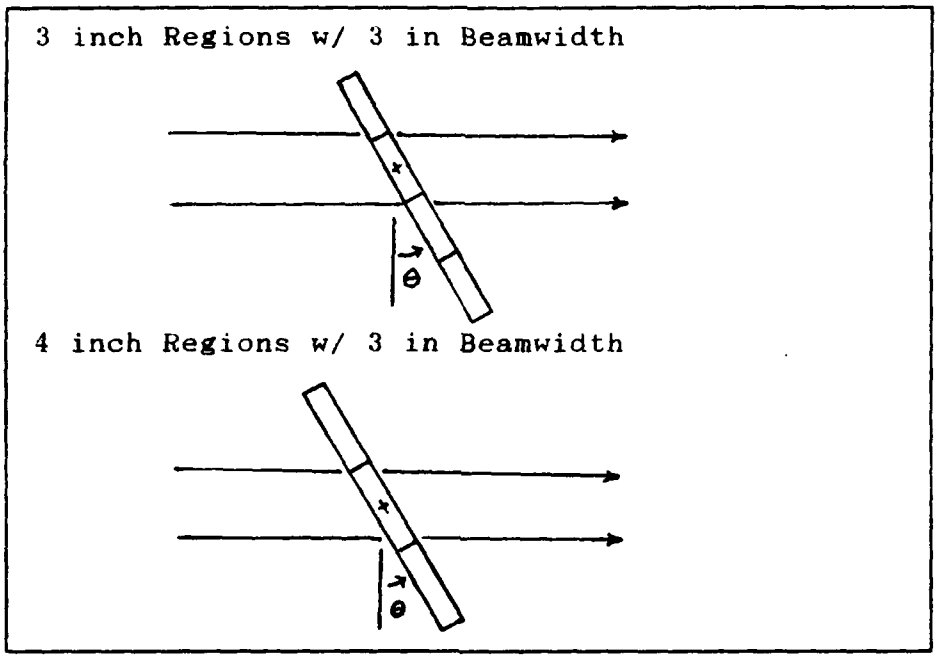

FIGURE 8. Beam Overlap Due To Incidence Angle

Once these distances were calculated, a support had to be built. It had to hold a foot square material sample on edge between the antennas and allow it to rotate through an axis which intersects the transmission axis. It also had to allow translation of the sample, both horizontally and vertically, to center any of the nine measurement areas on these two axis. These translation distances are the same as the center to center distance; four inches.

The necessary specifications for a framework which included three levels of movement was completed. An inner frame holds the material and can be moved to three positions, four inches apart, on two horizontal supports. The horizontal supports are mounted onto a middle frame, and can be shifted to three positions, four

inches apart vertically. The center of the middle frame is pinned at the top and bottom to the outer frame which allows it to rotate through a vertical axis. The outer frame also provides all of the support for the entire structure. A picture of the support constructed is shown in Figure 9.

To finish the equipment setup, the various pieces needed only to be connected and positioned. The antenna mounts used by Joseph were modified to allow positioning at the correct height. The source, antennas, receiver, and all of the waveguide pieces were connected as shown in Figure 10.

The final setup used a Scientific Atlanta 1783 Programmable microwave receiver. A Scientific Atlanta 1784 and 1785 downconverter mixed the signals in two Hughes mixers with the

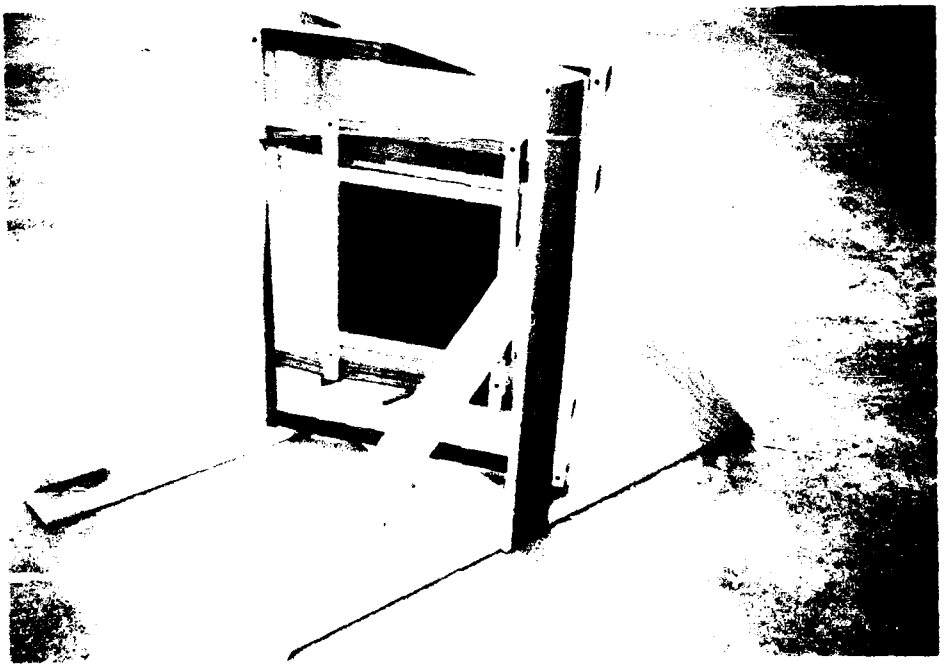

Figure 9. Material Support Frame

harmonics of a 11.25 GHz LO. Two Scientific Atlanta, single ended mixers convert the signal from the 2-4 GHz downconverter output to the 1-2 GHZ receiver band. Four Hughes isolators and a Hughes 10 dB directional coupler provided the necessary directional connections between the Hughes microwave source, the receiver, and two Alpha 856 Series, 3 inch diameter, horn lens antennas. All measurements were made in decibels and read as the difference between the reference and signal channel outputs. Prior to each measurement, the receiver's signals were zeroed with no material in the mount to set a reference level of 100% transmission and eliminate any noise, errors or losses from the system itself.

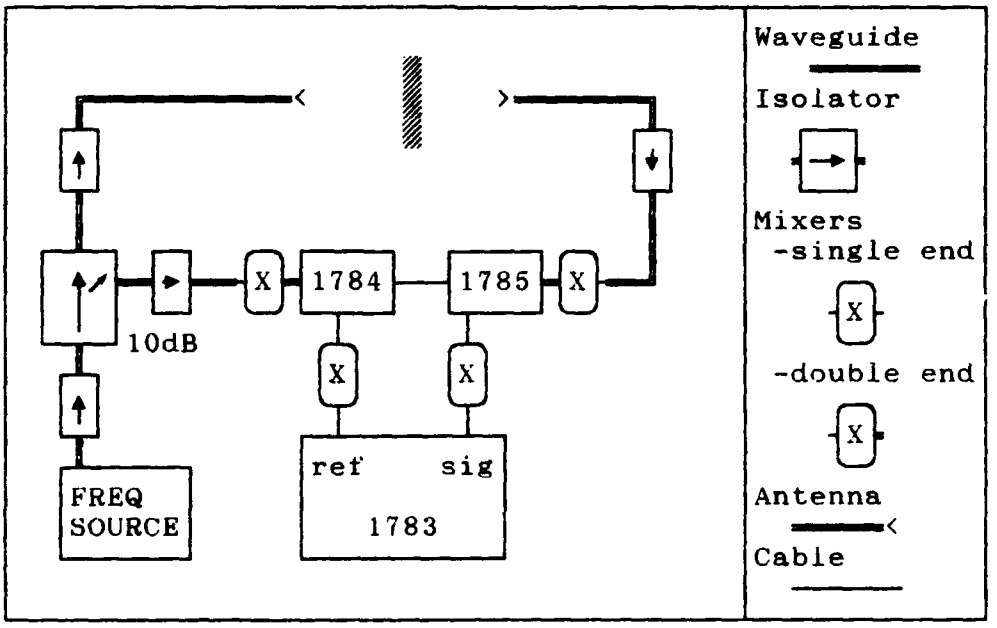

FIGURE 10. Equipment Setup

IV. Results

Introduction

This chapter reviews the work done to verify and demonstrate the performance of this free-space, parameter determination technique. It includes an explanation of some of the problems which were encountered and how they were dealt with, a review of the computer solution program, the results of applying the system towards evaluating both known and unknown values, and the testing of the system to locate intentionally planted "hot spots".

Problems and Changes

The only available antennas with a beamwidth narrow enough for these measurements were designed for operation at 56 GHz and 94 GHz. As the equipment was connected and tested, it was discovered that the California Microwaves 56 GHz source had some defective control devices, and the 94 GHz source was not stable enough for the receiver to lock on to. The defective devices of the 56 GHz source were replaced with those from the 94 GHz source, but because each device was so precisely calibrated for its own frequency, the exchanged pieces proved incompatible. Therefore, it was necessary to either find narrow beam antennas at a lower and more easily available frequency or other sources of either 56 or 94 GHz. The latter was achieved when the Avionics Laboratory (AFWAL/AAA) provided a similar 94 GHz source on loan.

Next came the task of establishing the spacing between the antennas. As was mentioned in the previous chapter, the spacing was to be a trade-off between the desire to remain in the close, undistorted, planar region of the antennas, and the need to separate the antennas far enough to reduce the standing wave between the direct and double-reflected components. As attempts were made to measure this standing wave, several problems arose.

First, the wavelength is approximately 3 millimeters at 94 GHz, so the repetition length of the standing wave is approximately 1.5 millimeters. It must be measured in increments smaller than .75 millimeters, equating to a sampling frequency of at least twice the frequency being measured. Second, although the supports and mounts for the antennas were built to be sturdy and rigid, they were not built with small, precise movement and narrow beam alignment in mind. These factors established a system in which it was very difficult to measure the standing wave. Every effort to move the antennas apart caused their alignment to change, and therefore it was indeterminable whether the change was from alignment or distance.

To defeat this difficulty, it was decided to establish what appeared to be an average, though arbitrarily determined, distance with the maintenance of the planar quality of the wave first in mind. This means the assumption must be made that the transmission power level and the attenuation due to the presence of the material sample will be sufficient to avoid any problems due to the standing wave.

The next problem was discovered when the first material samples were measured. Two pieces of fiberglass, approximately 1.4 millimeters thick were measured and the results initially appeared to be going as predicted; a slow monotonic decrease in the magnitude of the transmission coefficient with increasing incidence angle. This followed for five degree angle increments from ten to forty degrees at the three center and left vertical positions. But when measurements were attempted at the three right positions, the values dropped steeply, then rose almost to a unity value of zero decibels, and then began to drop again. The same thing continued in the right positions after rotating the sample within the mount, suggesting that it was not the samples but the support structure causing the problem.

The structure was then measured without a sample, but with the 14 inch square edge guards in place, and it was found that while the center and left positions varied only a few hundredths of a decibel, the right positions varied nearly half a decibel. It was also discovered that the antenna alignment was correlated to this effect, because the large variations could be switched from the right to the left vertical positions through slight movements of the antennas, although it could not be removed from both at the same time.

The effect was reduced by introducing two changes in the equipment setup. First, the antennas were moved from their original positions of 14 inches on either side of the material to 10 inches on either side. This was done to decrease the

interference between the radiated energy and the support, and to improve the planar quality of the fields. Second, a variable attenuator was installed between the frequency source and the coupler to introduce a means of amplitude control. Using this, the source's output power was decreased another 10 dB to compensate for the greater likelihood of a standing wave due to the antenna movement. Although the relative amplitudes between components would remain the same, this was an attempt to reduce the reflected components down to the receiver's noise level.

These changes had two effects on the measurement ability of the system. First, the measurable interference of the empty support was reduced to three or four hundredths of a decibel at all nine positions. This is a little more interference than was present at the unaffected positions prior to the changes, but at least it was uniform. The negative effect was that the maximum angle of incidence had to be reduced to prevent the material support from coming in contact with the antenna mounts. The new maximum angle of incidence was set at 25 degrees.

Computer Program Evaluation

Code Development. The need for a computer program to convert the transmission measurements into the bulk parameter values was as important as the need for the measurement equipment itself. The end result could not be achieved without either of these two tools. The previous work done by Joseph provided several slightly different versions of the same main

program, utilizing a steepest descent algorithm to solve the resultant nonlinear system of equations. The differences between the programs was due to the choice of polarization and the quality of the material; nonmagnetic or nonmagnetic and lossless.

At first, efforts were made to check and test these programs, making corrections when necessary in order to improve them. The programs which solved for all four parameters were kept, as any simpler program could be derived from these. A few errors were found and corrected in the algorithm. Then, a number of equations were expanded, regrouped, and simplified to make use of the fact that several quantities are recurring. However, the final system did not work any better than the original.

So, the problem was approached from another angle. The derivatives of the transmission equation were rederived using complex algebra. These equations allowed use of FORTRAN's inherent ability to do complex calculations in the evaluation subroutine, and are reviewed in Appendix A. They are also different in that they calculate the magnitude of T, not $|T|^2$ as Joseph did, and incorporate both polarizations in a single set of equations. The steepest descent loop and gradient calculating subroutine was rewritten to take advantage of this capability.

The program was further improved to include a second technique for the solution of a system of nonlinear equations. This technique, called the Newton method, required the same calculations as the steepest descent method and is a faster

technique, but must have a good approximation as a starting point. The total program was configured to allow direct access to the Newton method, should a good approximation already be known. It also allowed the steepest descent results to be transferred to and tried by the Newton method, with the provision that if the Newton method diverged, the steepest descent method could be resumed from the same point and with the same values as when it had been left.

The program was also upgraded to allow the input of any prior qualitative knowledge of the material. For the nonmagnetic case, the system sets the permeability equal to free-space, sets its derivatives to zero, and reduces the system requirements to two equations with two unknowns. Further categorization of the material as lossless sets the imaginary permittivity component and its derivative to zero, and reduces the system to one equation with one unknown.

The steepest descent loop continues until either a maximum iteration number or a tolerance level is achieved. At these break points, the present solution values can be tried in the Newton method. Other choices at these break points include increasing the maximum iteration level or decreasing the tolerance level and reentering the steepest descent loop, or restarting the program, making use of as many repetitive inputs as possible.

The next improvement was to include a self-test option. This option allows the program to accept a set of solution

parameters, from which it calculates transmission coefficients and stores in the variables normally used for the measured coefficients. Then, it accepts a set of starting values for the parameters and tries to change them into the correct values using the normal algorithmic steps. Finally, with all of these aspects of the program running correctly, the answers were compared with Joseph's for self-tests covering several possible measurement situations. The final program is reviewed in Appendix B.

Self-Testing. The final version of the computer program was self-tested for several material examples. The following vectors are defined to aid in examining these test results:

$\underline{X}$: a set of relative parameter values; $[\epsilon', \epsilon'', \mu', \mu'']$

$\underline{A}$: a set of incidence angles in degrees; $[\theta_1, \theta_2, \theta_3, \theta_4]$

The results of the first self-test are shown in Table I and are compared with Joseph's results using his final programs. They were run for a frequency of 94 GHz, $\underline{A}$ = [0, 20, 40, 60], and a thickness of 0.254 cm (0.1 in). The initial values were $\underline{X}$ = [4, 0.5, 1, 0.5]. The iteration column describes how long it took the present computer program to derive its solution in numbers of steepest descent and Newton iterations.

Table II reviews additional self-testing for the program. The same solution set $\underline{X}$ = [5, 1, 2, 1] and starting point $\underline{X}$ = [4, 0.5, 1, 0.5] were used, but different combinations of frequency,

Table I

Results of Self-Test # 1

Polarization	Solution Values $\underline{X}$	Joseph's Results	Present Results	Iterations (S.D./N.)
Perpendicular	5.0	4.215	5.000	
	1.0	0.534	1.000	20 S. D.
	2.0	1.933	2.000	5 N.
	1.0	1.294	1.000	
Parallel	5.0	5.064	5.000	
	1.0	0.547	1.000	1 S. D.
	2.0	1.839	2.000	5 N.
	1.0	1.163	1.000	

thickness and angles were set. The angle sets were $\underline{A}1$ = [0, 20, 40, 60] and $\underline{A}2$ = [10, 15, 20, 25]. The exact solution set was achieved in each case, differing only in the iterations required.

The self-tests revealed several interesting facts. Test 1 demonstrated the improvement of this code over the previous versions. Test 2 was an effort to examine how the solution time was affected by each of the external parameters; frequency, thickness, incidence angles, and polarization. In most cases, the program solved the test more quickly for a lower frequency and for parallel polarization. The program also tended to solve thinner sample tests more quickly, which may be due to the difference between the solution and starting point transmission coefficients would be greater for a thicker material sample, and so more correction would be required. The greatest solution difference was due to the degree to which the angles were spread apart. A larger spread produces a larger difference between each

Table II

Results of Self-Test # 2

Freq. GHz		Thickness cm		Angles		Iterations	
94	56	0.254	1.0	A1	A2	Perp. Pol.	Parl. Pol.
X		X		X		20 SD/ 5 N	1 SD/ 5 N
X		X			X	23 SD/10 N	400 SD/10 N
X			X	X		20 SD/ 5 N	9 SD/ 4 N
X			X		X	3200 SD/ 8 N	2200 SD/ 9 N
	X	X		X		52 SD/ 6 N	1 SD/ 4 N
	X	X			X	1 SD/ 6 N	1 SD/ 6 N
	X		X	X		16 SD/ 4 N	6 SD/ 3 N
	X		X		X	1800 SD/ 6 N	200 SD/ 8 N

angle's transmission value, resulting in a more diverse amount of information from which the guess is corrected.

Exceptions to all of these observations are noticeable in just the few tests done. The interactions between all of these factors, as well as the choice of solution and starting values, are so complex that any rules of thumb must be vague and are often incorrect. Another factor to keep in mind when comparing solutions by the iterations is the fact that once a solution is achieved for one measurement area, it can be used as the starting values for the other eight areas. These solutions should require fewer iterations because the starting value is much more accurate than the starting values for the first area. This leads to the next test, which was an examination of the effects of variance and error from one measurement to the next.

Given the degree of accuracy that the first and second test solutions had, the third test examined the effects if these

solutions were used as starting points for the next area's transmission measurements which were off by five percent. The solution values were set to $\underline{X}$ = [5, 1, 2, 1], and then the coefficients were adjusted plus or minus five percent. The other conditions were 94 GHz, 0.254 cm and $\underline{A}$ = [10, 15, 20, 25]. The results for this test are shown on Table III. Again, the parallel case seemed to provide the most accurate values for the least iterations, but it also contained the term with the most error; the imaginary permeability value. No Newton iterations were recorded because the steepest descent method could not get solutions accurate enough that it would not diverge.

Known Measured Values

To evaluate the final program's ability to solve real problems, measurements of several known and unknown materials were conducted. The known materials are those whose parameters

Table III

Results of Self-Test # 3

Polarization	Solution and Start Values $\underline{X}$	Plus 5% Solution Values $\underline{X}$	Minus 5% Solution Values $\underline{X}$	Iterations (S.D./N.)
Perpendicular	5.0	5.2411	5.0029	
	1.0	1.0643	0.9689	500 S. D.
	2.0	1.9126	2.0648	0 N.
	1.0	1.0168	0.9481	
Parallel	5.0	5.0278	4.9673	
	1.0	1.0276	0.9720	100 S. D.
	2.0	2.0080	1.9902	0 N.
	1.0	1.0616	0.9389	

are known to some degree prior to actual measurement. The purpose for measuring known materials is to provide a means of checking the measurement system's accuracy.

The first known materials measured were two pieces of fiberglass. Fiberglass is a nonmagnetic, lossless material, therefore only the real component of the permittivity needed to be evaluated. Although this would seem a simple process, to solve one equation for one unknown, the transmission coefficient varies with respect to real permittivity as shown in Figure 11. A solution would be the value where a horizontal line drawn at the measured transmission value intersects this function. It is

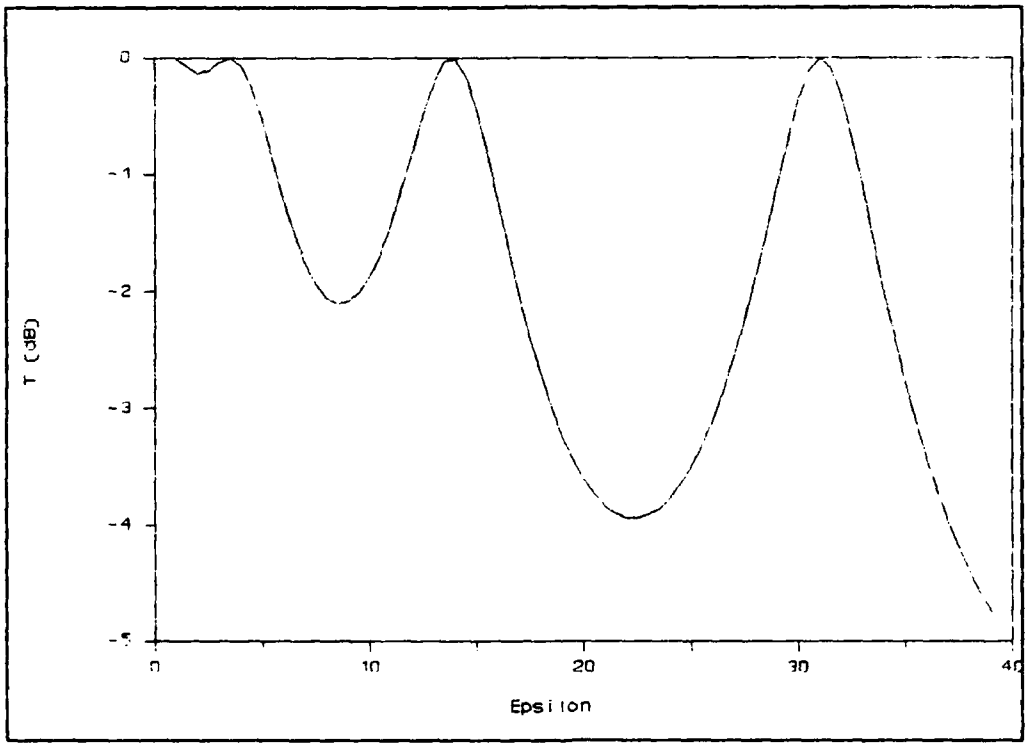

Figure 11. Transmission Coefficient Vs. Epsilon

apparent that for a specific frequency, thickness, and angle, there can be many sclutions. The solution produced by a computer code would depend then on the initial guessed value.

For this reason, although only one measurement at one angle is necessary to obtain a solution, several measurements at different angles may be required to obtain the unique solution. Figure 12 shows several plots at different angles, and plotted measured transmission coefficients. In this example, the only value which intersects all of the angular plots at their respective transmission coefficients is three. It must be the unique solution.

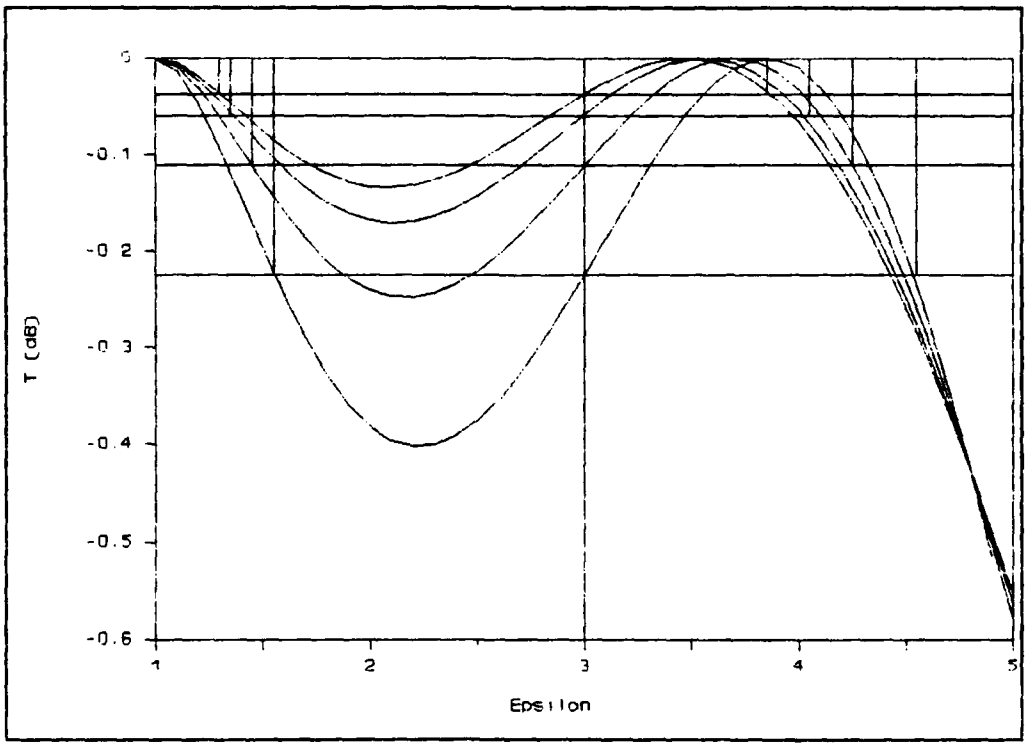

Figure 12. Unique Solution Example

To avoid multiple solutions, each piece of fiberglass was measured at four angles of incidence; $\underline{A}$ = [10, 15, 20, 25] in degrees. The measured values are listed in Table IV.

The previous knowledge of the permittivity of fiberglass was limited. A copy of the measured values in the 12-18 GHz range suggests an average permittivity value of approximately 4.5 in this band, see Figure 13. It appears that the permittivity of fiberglass does not vary much with frequency, therefore 4.5 was chosen as a starting value for the computer program. Table V lists the permittivity values obtained from each transmission coefficient. From this data, an average permittivity value for each sheet was calculated as 6.7736 and 6.9181, with standard deviations of 0.039 and 0.054, respectively. If these values were assumed correct, the greatest measurement error was 1.4 %.

Table IV

Fiberglass Transmission Measurements (dB)

Vertical Position and Angle		Horizontal Position (Sample 1/Sample 2)		
		Left	Center	Right
Top	10	-1.10 / -1.19	-1.09 / -1.27	-1.13 / -1.16
	15	-1.17 / -1.28	-1.15 / -1.30	-1.19 / -1.21
	20	-1.28 / -1.38	-1.30 / -1.40	-1.31 / -1.31
	25	-1.40 / -1.51	-1.46 / -1.56	-1.49 / -1.52
Middle	10	-1.10 / -1.33	-1.10 / -1.25	-1.13 / -1.26
	15	-1.15 / -1.41	-1.18 / -1.30	-1.19 / -1.30
	20	-1.25 / -1.50	-1.29 / -1.45	-1.32 / -1.43
	25	-1.38 / -1.64	-1.44 / -1.62	-1.50 / -1.63
Bottom	10	-1.02 / -1.28	-1.08 / -1.31	-1.16 / -1.26
	15	-1.07 / -1.40	-1.14 / -1.39	-1.20 / -1.29
	20	-1.19 / -1.48	-1.29 / -1.48	-1.34 / -1.42
	25	-1.35 / -1.63	-1.44 / -1.64	-1.51 / -1.61

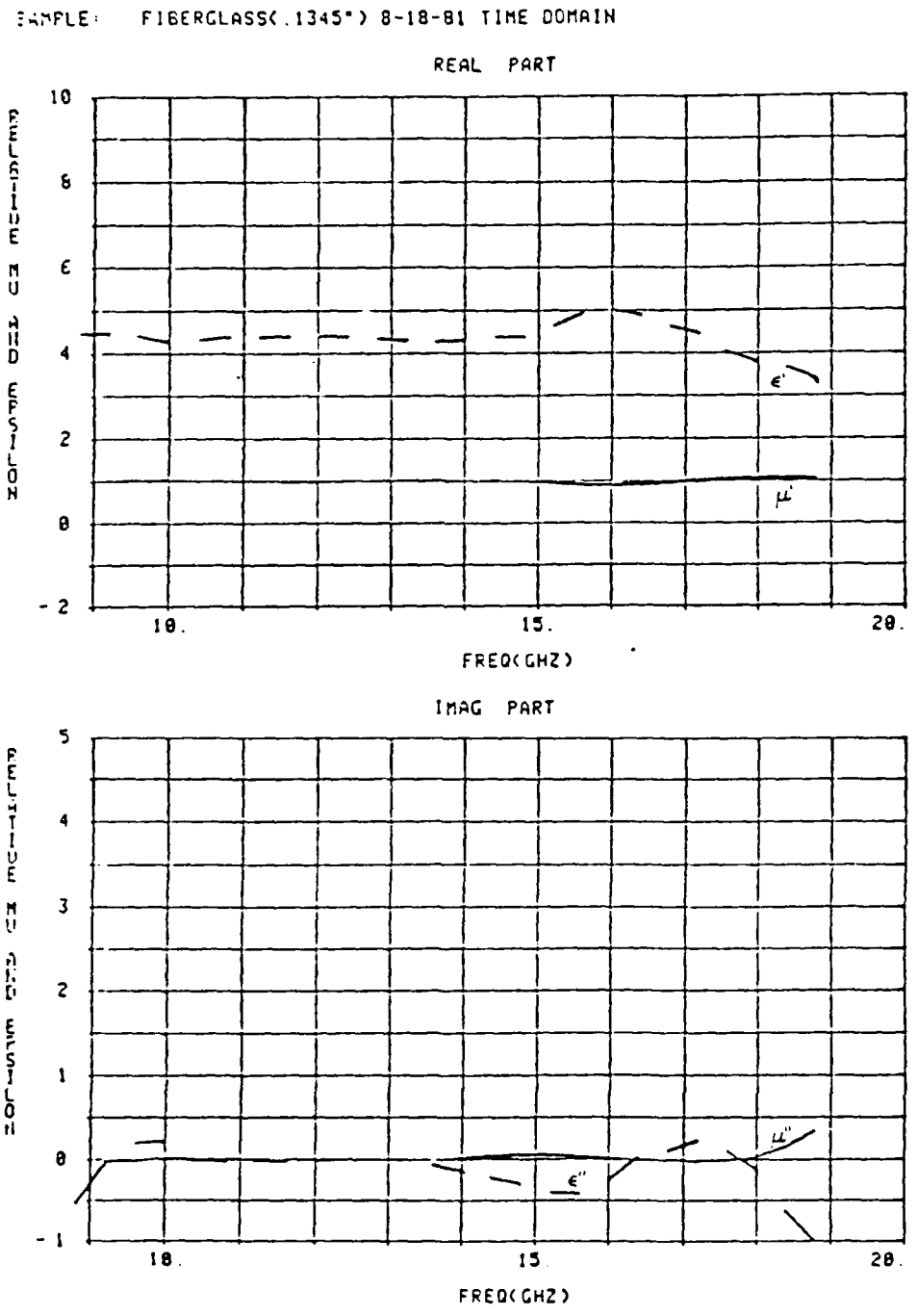

FIGURE 13. Mu-Epsilon of Fiberglass (Time Domain)

Table V

Fiberglass Permittivity Solutions

Vertical Position and Angle		Horizontal Position (Sample 1/Sample 2)		
		Left	Center	Right
Top	10	6.654 / 6.742	6.645 / 6.781	6.683 / 6.712
	15	6.714 / 6.819	6.696 / 6.838	6.733 / 6.752
	20	6.803 / 6.896	6.821 / 6.915	6.831 / 6.831
	25	6.889 / 6.987	6.942 / 7.033	6.969 / 6.996
Middle	10	6.654 / 6.883	6.654 / 6.801	6.683 / 6.811
	15	6.696 / 6.948	6.724 / 6.838	6.733 / 6.838
	20	6.776 / 7.012	6.812 / 6.963	6.840 / 6.944
	25	6.871 / 7.110	6.924 / 7.091	6.978 / 7.100
Bottom	10	6.579 / 6.831	6.635 / 6.862	6.712 / 6.811
	15	6.622 / 6.938	6.686 / 6.928	6.742 / 6.829
	20	6.722 / 6.992	6.812 / 6.992	6.858 / 6.934
	25	6.845 / 7.100	6.924 / 7.110	6.987 / 7.081

The next material measured was a piece of plexiglass; a nonmagnetic, lossless material which is known to have a permittivity close to 2.6 at microwave frequencies (10:51). The piece measured was only 12 inches by 12 inches, which is the same as the inside dimensions of the innermost material frames, so some small pieces of tape were used around the edges to hold it in place. Their effect was assumed to be negligible.

The sample also had a small rectangular piece of one corner missing, measuring 1.25 inches wide by 2.125 inches high. This sample was chosen so that not only could the accuracy of the measurement system be tested, but so the effect that a defect in one measurement area has on its surrounding areas could also be

examined. The transmission measurements are listed in Table VI, and the solutions obtained from them are listed in Table VII.

If the permittivity of plexiglass was exactly 2.6 at 94 GHz, the error in any of the non-defective areas ranged from 0.3 to 6.5 %, while errors in the defective area ranged from 13 to 77 %. As expected, the maximum error occurs at the smallest angle of incidence, where the largest projected area of the defect is visible. The average of the non-defective area measurements was 2.68 (standard deviation; 0.050). If this value was assumed correct at 94 GHz, the maximum error of these eight regions was 3.3 %, while the defective region erred from 9.7 to 72 %.

It appears that this defect had little effect upon any of the surrounding areas. This supports the assumption that each

Table VI

Plexiglass Measurements (dB)

Vertical Position and Angle		Horizontal Position		
		Left	Center	Right
Top	10	- 0.73	- 0.20	- 0.18
	15	- 0.65	- 0.20	- 0.18
	20	- 0.59	- 0.21	- 0.18
	25	- 0.54	- 0.26	- 0.21
Middle	10	- 0.21	- 0.21	- 0.19
	15	- 0.20	- 0.21	- 0.19
	20	- 0.21	- 0.21	- 0.20
	25	- 0.27	- 0.26	- 0.23
Bottom	10	- 0.22	- 0.22	- 0.21
	15	- 0.21	- 0.21	- 0.22
	20	- 0.21	- 0.22	- 0.22
	25	- 0.26	- 0.26	- 0.25

Table VII

Plexiglass Permittivity Solutions

Vertical Position and Angle		Horizontal Position		
		Left	Center	Right
Top	10	4.61634	2.62518	2.60732
	15	3.02146	2.64824	2.63114
	20	2.96217	2.68814	2.66427
	25	2.94028	2.76280	2.72819
Middle	10	2.63393	2.63393	2.61630
	15	2.64824	2.65659	2.63977
	20	2.68814	2.68814	2.68032
	25	2.76948	2.76280	2.74231
Bottom	10	2.64257	2.64257	2.63393
	15	2.65659	2.65659	2.66483
	20	2.68814	2.69584	2.69584
	25	2.76280	2.76280	2.75605

region could be assumed locally homogeneous because the surrounding regions would contribute negligibly to its power measurement. However, this isolation effect could be exaggerated due to the position of the defect on the outer edge of the region, furthest from any neighboring regions. Measurements taken under the heading of intentionally placed "hot spots" will examine this effect further.

Unknown Measured Values

Two unknown materials were also measured. The first was a nonmagnetic, lossy absorber made by Advanced Absorber Products called AAP-ML-73. The parameters of interest were the real and imaginary permittivity values. Again, only measurements at two

angles were required for a solution, yet measurements were taken at four angles, processed for each angle pair combination, and averaged. The measurements are recorded in Table VIII, and the average solution values are in Table IX, with standard deviations in parenthesis. Appendix C has all the solutions per angle pair.

It is known that the real component of the permittivity can never be less than one, yet two of the solution values are less than one. This is because the solution program does not yet take this restriction into account. Since the solution values are each only slightly less than one, these are probably only due to some error in the measurement process. For example, this material is very spongy and porous. The error could be due to a variation in the thickness, either due to manufacture or due to that edge being over-tightened in the support.

Table VIII

AAP-ML-73 Measurements (dB)

Vertical Position and Angle		Horizontal Position		
		Left	Center	Right
Top	10	-29.20	-30.82	-29.03
	15	-29.41	-31.19	-29.45
	20	-29.85	-31.72	-30.14
	25	-30.52	-32.53	-31.11
Middle	10	-29.92	-29.36	-28.09
	15	-30.32	-29.77	-28.47
	20	-30.89	-30.28	-29.16
	25	-31.62	-31.09	-30.06
Bottom	10	-25.53	-27.98	-29.52
	15	-25.77	-28.34	-29.84
	20	-26.21	-28.87	-30.49
	25	-26.92	-29.54	-31.37

Table IX

AAP-ML-73 Parameters

Vertical Position and Angle	Horizontal Position		
	Left	Center	Right
Top ϵ'	1.639 (0.478)	1.128 (0.104)	0.840 (0.090)
ϵ''	1.055 (0.136)	0.958 (0.040)	0.787 (0.037)
Middle ϵ'	1.083 (0.007)	1.075 (0.096)	0.885 (0.118)
ϵ''	0.912 (0.003)	0.889 (0.036)	0.775 (0.044)
Bottom ϵ'	1.340 (0.285)	1.157 (0.020)	1.015 (0.223)
ϵ''	0.835 (0.082)	0.870 (0.007)	0.867 (0.080)

The other unknown material measured was a piece of magnetic absorber. Because the material was nonrigid, it was sandwiched between the two pieces of fiberglass measured earlier to allow proper mounting. The measurements at each of the four angles produced a solution set of four bulk parameter values. The measurements are in Table X; two solution sets are in Table XI.

This demonstrates that multiple solution sets are also possible when solving for all four parameters, just as they were when solving for only one parameter. When solving for two parameters, the same solution was achieved regardless of the starting point, although this does not mean they do not exist in this case. Both sets were averaged over the nine areas, and the averages and standard deviations were $\underline{X}_1$ = [4.901, 1.500, 0.068, 0.107], σ_1 = [0.001,0.0004,0.024,0.029] and $\underline{X}_2$ = [4.468, 0.909, 0.063, 0.132], σ_2 = [0.023,0.004,0.026,0.034]. The first set, having the least variation, will be assumed the correct solution.

Table X

Magnetic Material Measurements (dB)

Vertical Position and Angle		Horizontal Position		
		Left	Center	Right
Top	10	-19.61	-19.96	-20.12
	15	-20.09	-20.66	-20.58
	20	-20.69	-21.65	-21.36
	25	-21.41	-22.86	-22.42
Middle	10	-16.31	-18.37	-18.91
	15	-16.80	-19.12	-19.41
	20	-17.59	-20.17	-20.14
	25	-18.70	-21.46	-21.33
Bottom	10	-23.32	-21.19	-18.43
	15	-23.90	-21.76	-18.82
	20	-24.53	-22.55	-19.38
	25	-25.31	-23.56	-20.32

Table XI

Magnetic Material Parameters

Vertical Position and Angle		Horizontal Position (Sol.1 / Sol.2)		
		Left	Center	Right
Top	ϵ'	4.902 / 4.451	4.898 / 4.498	4.901 / 4.501
	ϵ''	1.500 / 0.910	1.500 / 0.911	1.500 / 0.910
	μ'	0.107 / 0.106	0.037 / 0.029	0.065 / 0.059
	μ''	0.126 / 0.158	0.093 / 0.112	0.112 / 0.136
Middle	ϵ'	4.900 / 4.498	4.900 / 4.453	4.900 / 4.454
	ϵ''	1.499 / 0.898	1.500 / 0.910	1.500 / 0.910
	μ'	0.064 / 0.064	0.037 / 0.031	0.062 / 0.058
	μ''	0.070 / 0.090	0.076 / 0.094	0.096 / 0.120
Bottom	ϵ'	4.902 / 4.452	4.901 / 4.452	4.902 / 4.455
	ϵ''	1.500 / 0.910	1.500 / 0.910	1.499 / 0.909
	μ'	0.085 / 0.072	0.058 / 0.049	0.096 / 0.097
	μ''	0.165 / 0.198	0.121 / 0.147	0.107 / 0.135

Intentional "Hot Spot" Measurement

The effect of "hot spots", or defective regions, has already been mentioned during the plexiglass measurement. The question of whether or not this measurement technique can identify a region whose qualities vary greatly from the rest was tested next. Unfortunately, producing specific variances in the parameter values of only one region, for comparison to the others, cannot be done exactly. Substituting a different material into one region could be done. This was decided against because of the possibility of unwanted effects due to the discontinuity between materials and the inability to secure regional boundaries except at the outermost edges.

The method chosen was to physically alter the material in one region. The exact effect is not to change the parameters but to change the material qualities which are maintained as constants by the computer program. Therefore, the program forces the parameters to change to account for the changes in these values, which it is not informed of, and the same desired results are obtained.

The AAP-ML-73 material sample was tested, and the first alteration was to tape a one inch square piece of aluminum foil to the center of the middle, right measurement region. The measurements plainly show a defect since they are two to three decibels lower than in the unaltered case, as shown in Table XII.

The solution values are presented as they were for the unaltered case, with the listing of all of the solutions for each

angle pairing in Appendix C, and the averages for each area in Table XIII. The effect was an increase in parameter values by approximately 0.25 in the altered region, and a change of approximately 0.1 in the other regions, with decreases in most.

Table XII

Foiled AAP-ML-73 Measurements (dB)

Vertical Position and Angle		Horizontal Position		
		Left	Center	Right
Top	10	-28.92	-30.85	-28.96
	15	-29.31	-31.14	-29.40
	20	-29.65	-31.77	-30.19
	25	-30.33	-32.55	-31.11
Middle	10	-29.70	-29.14	-32.31
	15	-30.02	-29.57	-32.69
	20	-30.54	-30.21	-33.25
	25	-31.20	-31.04	-34.05
Bottom	10	-25.01	-27.66	-29.40
	15	-25.28	-28.04	-29.83
	20	-25.71	-28.62	-30.41
	25	-26.36	-29.40	-31.38

Table XIII

Foiled AAP-ML-73 Parameters

Vertical Position and Angle		Horizontal Position		
		Left	Center	Right
Top	ϵ'	1.430 (0.330)	1.157 (0.277)	0.785 (0.085)
	ϵ''	0.988 (0.102)	0.965 (0.096)	0.764 (0.036)
Middle	ϵ'	1.277 (0.090)	0.927 (0.022)	1.122 (0.080)
	ϵ''	0.971 (0.030)	0.827 (0.009)	1.010 (0.032)
Bottom	ϵ'	1.316 (0.153)	1.013 (0.048)	0.918 (0.110)
	ϵ''	0.813 (0.045)	0.810 (0.017)	0.830 (0.046)

Next, a block of material was cut from the center of the same region, approximately 3/8" on a side and extending halfway into the sample. After the sample was measured, the remaining material was removed to produce a 3/8" hole completely through the sample and it was measured again. Both times, the measurements appear as if there is no defect, being bounded by both larger and smaller measurements in other areas, see Tables XIV and XV. However, the solution values obtained from these tests clearly show the effects of these holes, as listed in Tables XVI and XVII.

The final "hot spot" test done with the sample of AAP-ML-73 was prepared by pouring water into the center of the lower, middle region. After the water was absorbed, the sample was

Table XIV

Half Hole AAP-ML-73 Measurements (dB)

Vertical Position and Angle		Horizontal Position		
		Left	Center	Right
Top	10	-29.14	-30.90	-28.87
	15	-29.42	-31.23	-29.36
	20	-29.87	-31.83	-30.19
	25	-30.43	-32.65	-31.17
Middle	10	-29.62	-29.15	-26.73
	15	-30.04	-29.70	-27.22
	20	-30.58	-30.22	-28.03
	25	-31.32	-31.02	-28.91
Bottom	10	-25.10	-27.74	-29.31
	15	-25.42	-28.05	-29.83
	20	-25.82	-28.65	-30.46
	25	-26.54	-29.54	-31.33

Table XV

Whole Hole AAP-ML-73 Measurements (dB)

Vertical Position and Angle		Horizontal Position		
		Left	Center	Right
Top	10	-29.15	-30.88	-28.94
	15	-29.52	-31.30	-29.56
	20	-30.01	-31.88	-30.21
	25	-30.61	-32.67	-31.14
Middle	10	-29.63	-29.10	-26.72
	15	-30.01	-29.52	-27.63
	20	-30.61	-30.22	-28.73
	25	-31.30	-31.03	-30.02
Bottom	10	-25.07	-27.72	-29.55
	15	-25.35	-28.16	-29.98
	20	-25.81	-28.81	-30.55
	25	-26.48	-29.52	-31.48

Table XVI

Half Hole AAP-ML-73 Parameters

Vertical Position and Angle		Horizontal Position		
		Left	Center	Right
Top	ϵ'	1.516 (0.093)	1.103 (0.178)	0.712 (0.057)
	ϵ''	1.026 (0.028)	0.950 (0.065)	0.731 (0.026)
Middle	ϵ'	1.081 (0.044)	0.961 (0.166)	0.731 (0.065)
	ϵ''	0.901 (0.016)	0.840 (0.066)	0.676 (0.028)
Bottom	ϵ'	1.239 (0.165)	1.025 (0.220)	0.856 (0.062)
	ϵ''	0.794 (0.051)	0.811 (0.076)	0.806 (0.026)

Table XVII

Whole Hole AAP-ML-73 Parameters

Vertical Position and Angle	Horizontal Position		
	Left	Center	Right
Top ϵ'	1.283 (0.068)	1.038 (0.023)	0.762 (0.108)
ϵ''	0.954 (0.023)	0.928 (0.009)	0.756 (0.048)
Middle ϵ'	1.094 (0.063)	0.901 (0.066)	0.407 (0.071)
ϵ''	0.906 (0.024)	0.816 (0.027)	0.532 (0.041)
Bottom ϵ'	1.222 (0.140)	0.948 (0.081)	0.945 (0.099)
ϵ''	0.787 (0.041)	0.789 (0.031)	0.846 (0.041)

allowed to drain any excess water it could not hold before it was measured. Because there was already a hole in the side of this sample, only the altered region and its direct neighbors were measured. The measurements are listed in Table XVIII and the solutions in Table XIX.

In each "hot spot" test, the majority of the parameter values in the unaltered regions decreased by approximately a tenth in comparison to the original parameter measurements. The half hole test seems to produce a set of parameters only marginally recognizable as a defect since the real components are getting quite a bit below one, but the values do not stand out completely from the other regions.

The rest of the tests produce changes in parameter values that stand out from the other regions by several tenths. The foil and water both caused increased parameters and were also

quite noticeable from a simple inspection of the measured values. The holes both caused a decrease in the parameters, but were not so noticeable in the measured values.

Table XVIII

Wet AAP-ML-73 Measurements (dB)

Vertical Position and Angle	Horizontal Position		
	Left	Center	Right
Middle 10	------	-29.35	------
15	------	-29.76	------
20	------	-30.31	------
25	------	-31.02	------
Bottom 10	-25.09	-49.52	-29.49
15	-25.38	-50.26	-29.94
20	-25.78	-50.69	-30.47
25	-26.53	-51.17	-31.51

Table XIX

Wet AAP-ML-73 Parameters

Vertical Position and Angle	Horizontal Position		
	Left	Center	Right
Middle ϵ'	------	1.093 (0.032)	------
ϵ''	------	0.896 (0.017)	------
Bottom ϵ'	1.281 (0.200)	1.668 (0.908)	0.920 (0.172)
ϵ''	0.799 (0.065)	1.952 (0.477)	0.832 (0.071)

V. Conclusions and Recommendations

Review

This thesis was an effort to further the ability of making free-space constitutive parameter measurements. It attempted to expand upon previous work by improving the accuracy of the final parameter values, and more importantly by introducing the ability to examine the homogeneity of the material. This is very important because it will allow the examination of materials for "hot spots", or locations of large parameter variations from the average bulk values. This in turn will allow previously unknown material "hot spots" to be removed or replaced, avoiding their unwanted interactive effects before they can deteriorate the performance of any system of which they were part.

Conclusions

From the parameter values determined in the tests, the known cases, and the unknown cases, it is apparent that this technique is an improvement upon its predecessor. The tests showed that the original solution set could be calculated with a great degree of accuracy, usually with a small number of iterations. Although several hundred iterations were required in some cases, this should not have too much of a slowing effect on the calculation step of this process because once a solution is achieved at one measurement region, it can be used as the starting point for the other eight. The tests also showed that the error in the

obtained parameter values is on the same order as the error in the measurement system. This means that the errors grew very slowly while propagating through the computer program.

The measurements of known values demonstrated that the system was providing accurate material parameters. Although no material values were exactly known under the conditions that these were measured, the parameters obtained were close to expected from the available estimates. The unknown material measurements demonstrated the use of this technique as a method for obtaining data on materials. They also acted as references for comparison during the measurement of the "hot spots".

The "hot spots" measurements were not looking for accuracy as much as they were looking for the ability of this technique to identify defective regions. In every case where the parameters of one region varied by a few tenths from the rest, the region was identified. A change of one tenth roughly corresponds to ten percent, since most of the values were on the order of one. So, this technique has the ability to detect parameter variations on the order of ten to twenty percent from the average. This, in many cases, is better than the manufacturer's quote for expected variation. Thus, this technique is sure to detect any larger defects which would cause system problems.

Recommendations

There are still many ways that this system can be improved, expanded and simplified. The following is a list of suggestions for further research and development.

Accuracy Development

1) Redesign the mount and antenna support together to allow easier and more accurate antenna alignment and movement.
2) Redesign the mount for less interference between the mounting structure and the antenna's beam.
3) Analyze the antennas to understand and avoid their standing wave effects.
4) Analyze the antennas to evaluate and correct for the assumption of a planar wave in the near field.
5) Introduce a correction factor for the receiving antenna's increased power density due to the material (13:664).
6) Measure the bistatic reflection coefficient to eliminate the standing wave problems.

Expansion

1) Introduce magnitude and phase measurement capability as a step towards the ability to convert data to the time domain to allow diagnostic imaging.
2) Convert to spread spectrum frequency measurements, as another requirement for time domain analysis.

Simplification

1) Use nonlinear regression as a solution technique to allow use of all points at once.

2) Redesign the support for easier positioning and placement of the samples.

3) Double the number of equations to reduce the number of required measurement angles by

   A) Introducing the capability to easily switch polarization, and measuring each sample at both.

   B) Introducing the capability to measure the bistatic reflection coefficient, while maintaining the transmission measurements.

   C) Introducing the capability to measure both the magnitude and phase.

   If the number of angles can be reduced to only one, the material support can be redesigned without the need to rotate, only translate, and therefore be much more stable.

Many of these ideas, such as redesign of the support, are repeated with emphasis on different aspects of the system. Therefore, a combination of only a few of these recommendations can produce a substantial system improvement if each is developed fully.

Appendix A: Complex Transmission Equations

$$T = 2 \,/\, (2\cos(d) + j(Z+1/Z)\sin(d)) \tag{A1}$$

The magnitude of the transmission coefficient can be expressed in several ways.

$$Tm = | T | = TM^{1/2} \tag{A2}$$

where

$$TM = TT^* \tag{A3}$$

Expressed in decibels:

$$TD = 10\log_{10}(Tm) = 5\log_{10}(TM) \tag{A4}$$

$$dTD/dx = 5\, d(\log_{10}(TM))/dx \tag{A5}$$

$$= 5\log_{10}e(1/TM)dTM/dx \tag{A6}$$

Deriving:

$$dTM/dx = d(TT^*)/dx = T(dT^*/dx)+T^*(dT/dx) \tag{A7}$$

$$= 2RE\{ T^*(dT/dx) \} \tag{A8}$$

$$dT/dx = T^2[(2\sin(d)-j(Z+1/Z)\cos(d))(dd/dx) - j(1-1/Z^2)\sin(d)(dZ/dx)]/2 \tag{A9}$$

$$dTM/dx = RE\{ T^* T^2[(2\sin(d)-j(Z+1/Z)\cos(d))(dd/dx) - j(1-1/Z^2)\sin(d)(dZ/dx)] \} \tag{A10}$$

$$dTM/dx = RE\{ TM\, T[(2\sin(d)-j(Z+1/Z)\cos(d))(dd/dx) - j(1-1/Z^2)\sin(d)(dZ/dx)] \} \tag{A11}$$

$$dTD/dx = 5\log_{10}e\ RE\{T[(2\sin(d)-j(Z+1/Z)\cos(d))(dd/dx) - j(1-1/Z^2)\sin(d)(dZ/dx)] \} \tag{A12}$$

$$d = 2\pi(d/l)[\epsilon_r\mu_r - \sin^2(o)]^{1/2} \quad (A13)$$

$$dd/dx = \pi(d/l)[\mu_r(d\epsilon_r/dx)+\epsilon_r(d\mu_r/dx)]/[\epsilon_r\mu_r-\sin^2(o)]^{1/2} \quad (A14)$$

For Perpendicular Case:

$$Z = \mu_r\cos(o)/[\epsilon_r\mu_r - \sin^2(o)]^{1/2} \quad (A15)$$

$$dZ/dx = -\cos(o)[\mu_r^2(d\epsilon_r/dx)+(2\sin^2(o)-\epsilon_r\mu_r)(d\mu_r/dx)] /2[\epsilon_r\mu_r-\sin^2(o)]^{3/2} \quad (A16)$$

For Parallel Case:

$$Z = [\epsilon_r\mu_r - \sin^2(o)]^{1/2}/\epsilon_r\cos(o) \quad (A17)$$

$$dZ/dx = [\epsilon_r^2(d\mu_r/dx)+(2\sin^2(o)-\epsilon_r\mu_r)(d\epsilon_r/dx)] /2\epsilon_r^2\cos(o)[\epsilon_r\mu_r-\sin^2(o)]^{1/2} \quad (A18)$$

Define:

$$I = [\epsilon_r\mu_r - \sin^2(o)]^{1/2} \quad (A19)$$

$$W4 = \pi(d/l) \quad (A20)$$

$$W1 = W4/I \quad (A21)$$

$$W2 = -\cos(o)/2I^3 \quad (A22)$$

$$W3 = 1/2\epsilon_r^2\cos(o)I \quad (A23)$$

PL = polarization flag = 1; perpedicular
0; parallel (A24)

Polynomials:

$$P1 = (2\sin(d)-j(Z+1/Z)\cos(d))W1 \quad (A25)$$

$$P2 = W2\mu_r^2PL + (2\sin^2(o)-\epsilon_r\mu_r)(1-PL)W3 \quad (A26)$$

$$P3 = W2(2\sin^2(o)-\epsilon_r\mu_r)PL + \epsilon_r^2(1-PL)W3 \quad (A27)$$

Then,

$$dTD/dx = 5\log_{10}e\ RE\{ T(P1[\mu_r(d\epsilon_r/dx)+\epsilon_r(d\mu_r/dx)] -j(1-1/Z^2)\sin(d)[P2(d\epsilon_r/dx)+P3(d\mu_r/dx)])) \quad (A28)$$

$$dTD/dx = RE\{ T(P1\mu_r-j(1-1/Z^2)\sin(d)P2)(d\epsilon_r/dx) +T(P1\epsilon_r-j(1-1/Z^2)\sin(d)P3)(d\mu_r/dx) \} \quad (A29)$$

Define Big Polynomials:

$$BP1 = T(P1\mu_r - j(1-1/Z^2)\sin(d)P2) \quad (A30)$$

$$BP2 = T(P1\epsilon_r - j(1-1/Z^2)\sin(d)P3) \quad (A31)$$

$$dTD/dx = RE\{ BP1(d\epsilon_r/dx) + BP2(d\mu_r/dx) \} \quad (A32)$$

Realizing that

$$\epsilon_r = \epsilon' - j\epsilon'' \quad (A33)$$

$$\mu_r = \mu' - j\mu'' \quad (A34)$$

$$d\epsilon_r/d\epsilon' = 1 \quad (A34)$$

$$d\epsilon_r/d\epsilon'' = -j \quad (A36)$$

$$d\epsilon_r/d\mu' = 0 \quad (A37)$$

$$d\epsilon_r/d\mu'' = 0 \quad (A38)$$

$$d\mu_r/d\epsilon' = 0 \quad (A39)$$

$$d\mu_r/d\epsilon'' = 0 \quad (A40)$$

$$d\mu_r/d\mu' = 1 \quad (A41)$$

$$d\mu_r/d\mu'' = -j \quad (A42)$$

$$dTD/d\epsilon' = RE\{ BP1(1) + BP2(0) \} = RE\{ BP1 \} \quad (A43)$$

$$dTD/d\epsilon'' = RE\{ BP1(-j) + BP2(0) \} = IM\{ BP1 \} \quad (A44)$$

$$dTD/d\mu' = RE\{ BP1(0) + BP2(1) \} = RE\{ BP2 \} \quad (A45)$$

$$dTD/d\mu'' = RE\{ BP1(0) + BP2(-j) \} = IM\{ BP2 \} \quad (A46)$$

Appendix B: Final Program with Self Test

Variables Used

Real

FR - Frequency (GHz)
PT - Material Thickness (cm)
PL - Incident Polarization Flag (Perp.=1,Parl.=2)
QA - Query Response (yes=1)
PI - π
W4 - $\pi(d/\lambda)$
QT - Test Flag (Test Mode =1)
DF - Derivative Flag; GRAD only calc. derivatives when DF=1
GG - Total Error; $\Sigma(TT-TA)^2$
Z0 - Magnitude of Gradient Vector
H1-H3 - Polynomial Coefficients for Solving A(4)
GF - Minimum Total Error Value
AF - Weight Corresponding To Minimum Total Error Value
YM - Magnitude of Correction Vector Y(x)
PVT - Pivot Check Value
TMP - Third Storage Variable for Pivoting
Q - Backsolution Sum
FN - Nonmagnetic Flag
FL - Lossless Flag
TOL - Switching Tolerance Level
TF - Tolerance Flag; TF=1 when ABS(GF-G(1))<TOL
EE - e=2.71828....

Integer

HH - Nonlinear System Order, Number of Equations
JJ,JK - Loop Counters
I,O - Loop Counters
K,KN - Iteration Counters, S.D. and Newton, respectively
KK,KKN - Additional Iterations, S.D. and Newton, respectively
MI,MIN - Maximum Iterations, S.D. and Newton, respectively
HM1 - HH-1
HP1 - HH+1
I - I+1
IPVT - Pivot Row Number

Complex

CJ - Imaginary Unit $j=(-1)$
E,CE - ϵ_r
U,CU - μ_r
ZE - Gradient Components for ϵ
ZU - Gradient Components for μ
I - Intermediate Term
D - Electrical Thickness
ZZ - Material Impedance
T - Transmission Coefficient
W1-W3 - Derivative Coefficients
P1-P3 - Derivative Polynomials
BP1,BP2 - Derivatives
TM - TT*

Arrays

TH(4) - Input Incidence Angles
X(4) - Input Parameter Values
TA(4) - Constant Transmission Coeff.; Measured or Self-Test Calc.
TT(4) - Variable Transmission Coeff.; Calc. from Guess Parameters
G(4) - Total Error for Guess Corrected by Weight A(x)
A(4) - Weights for Guessed Parameter Variation
Y(4) - Correction Term for Newton/Gauss Method
AN(4,5) - Augmented Jacobian Matrix
AR(4) - Augmentation Column; Total Error Values
TP(4) - Temporary Storage for ϵ,μ; Allows Return To Previous S.D. Values After Failed Newton Attempt

Flow Diagram of Program

Main Program

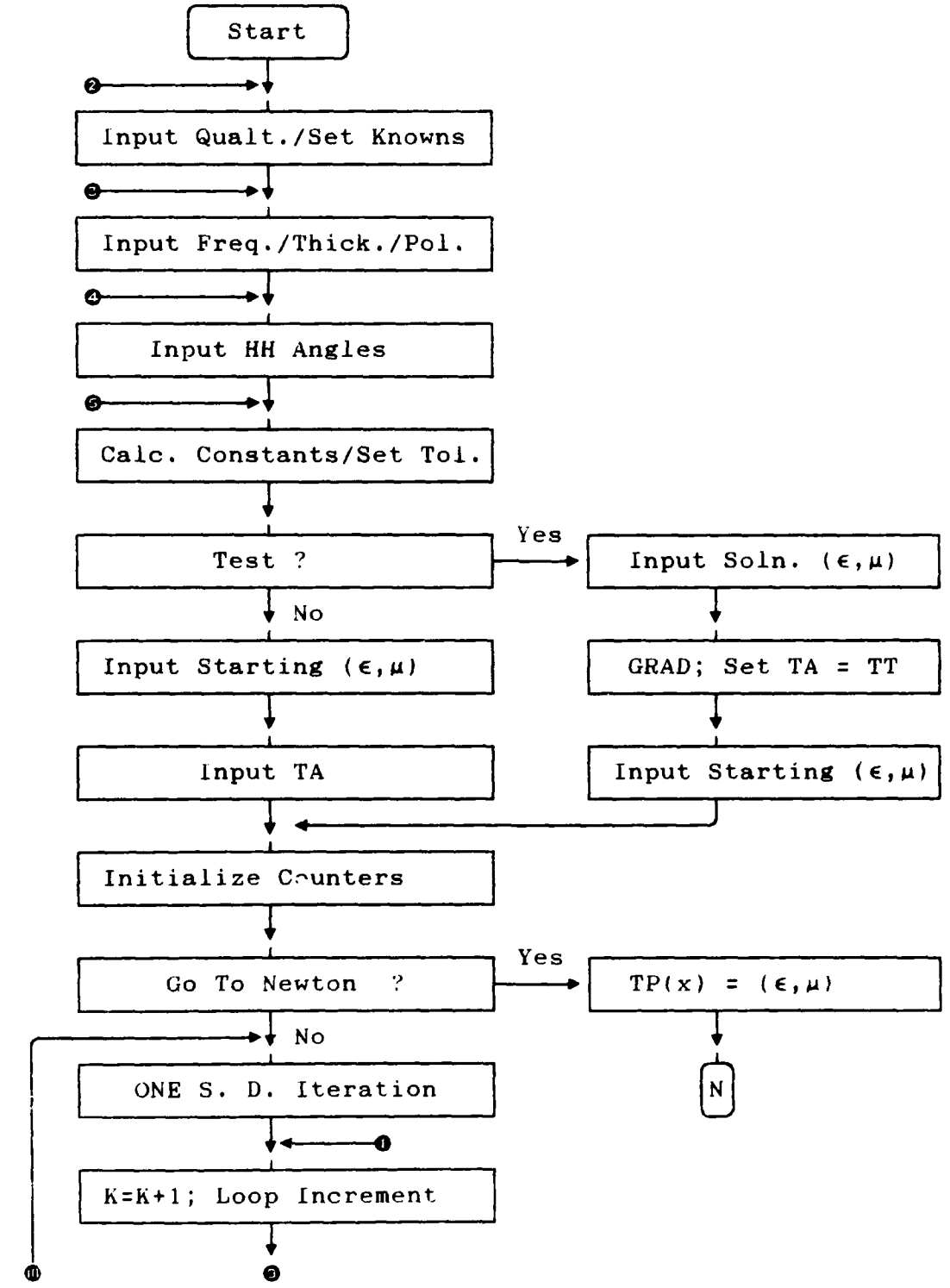

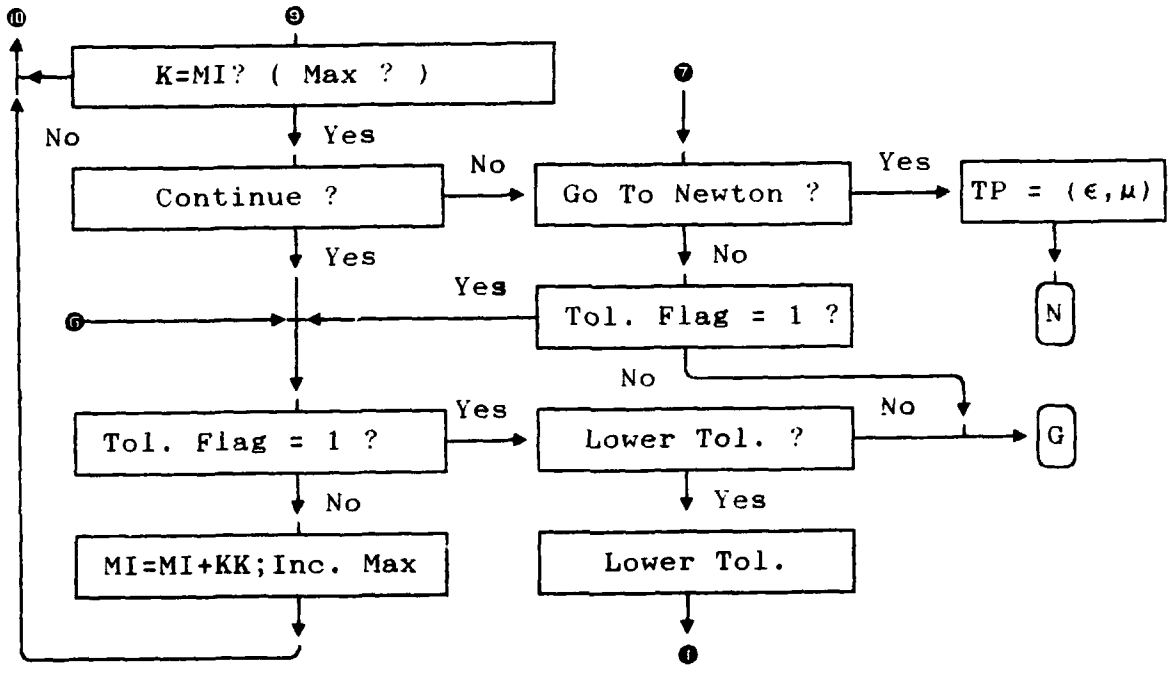
K=MI? (Max ?)
No
Yes
Continue ?
No
Go To Newton ?
Yes
TP = (ϵ,μ)
N
Yes
No
Yes
Tol. Flag = 1 ?
No
Tol. Flag = 1 ?
Yes
Lower Tol. ?
No
G
No
Yes
MI=MI+KK;Inc. Max
Lower Tol.

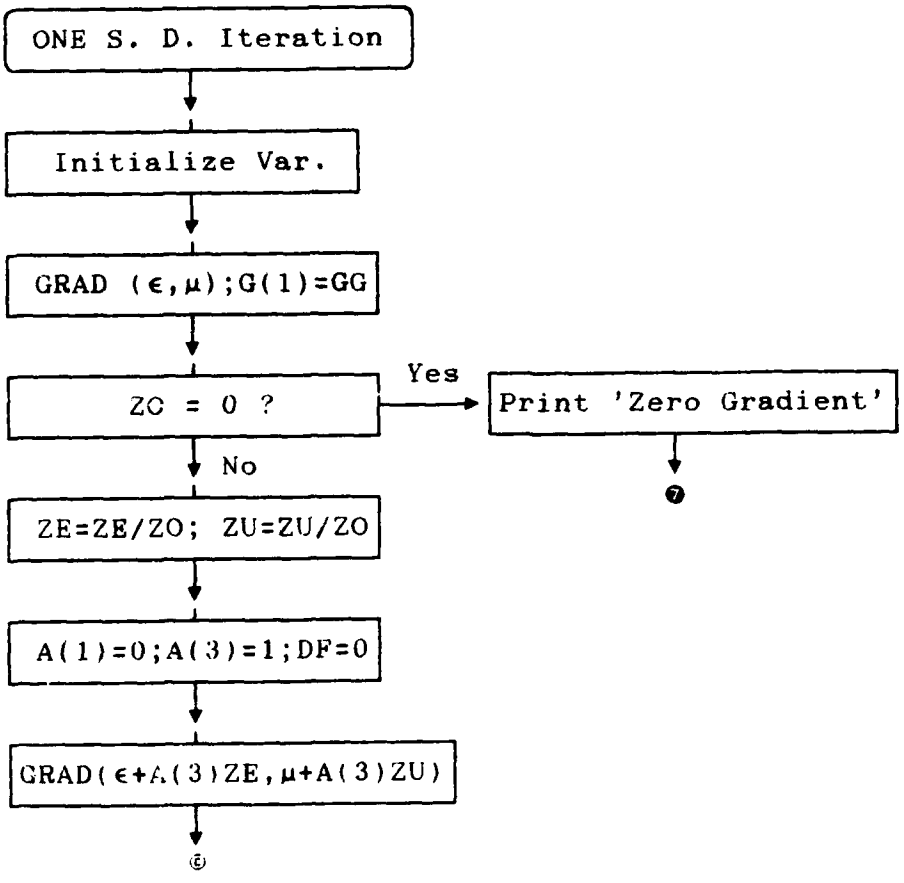
ONE S. D. Iteration
Initialize Var.
GRAD (ϵ,μ);G(1)=GG
ZC = 0 ?
Yes
Print 'Zero Gradient'
No
ZE=ZE/ZO; ZU=ZU/ZO
A(1)=0;A(3)=1;DF=0
GRAD(ϵ+A(3)ZE,μ+A(3)ZU)

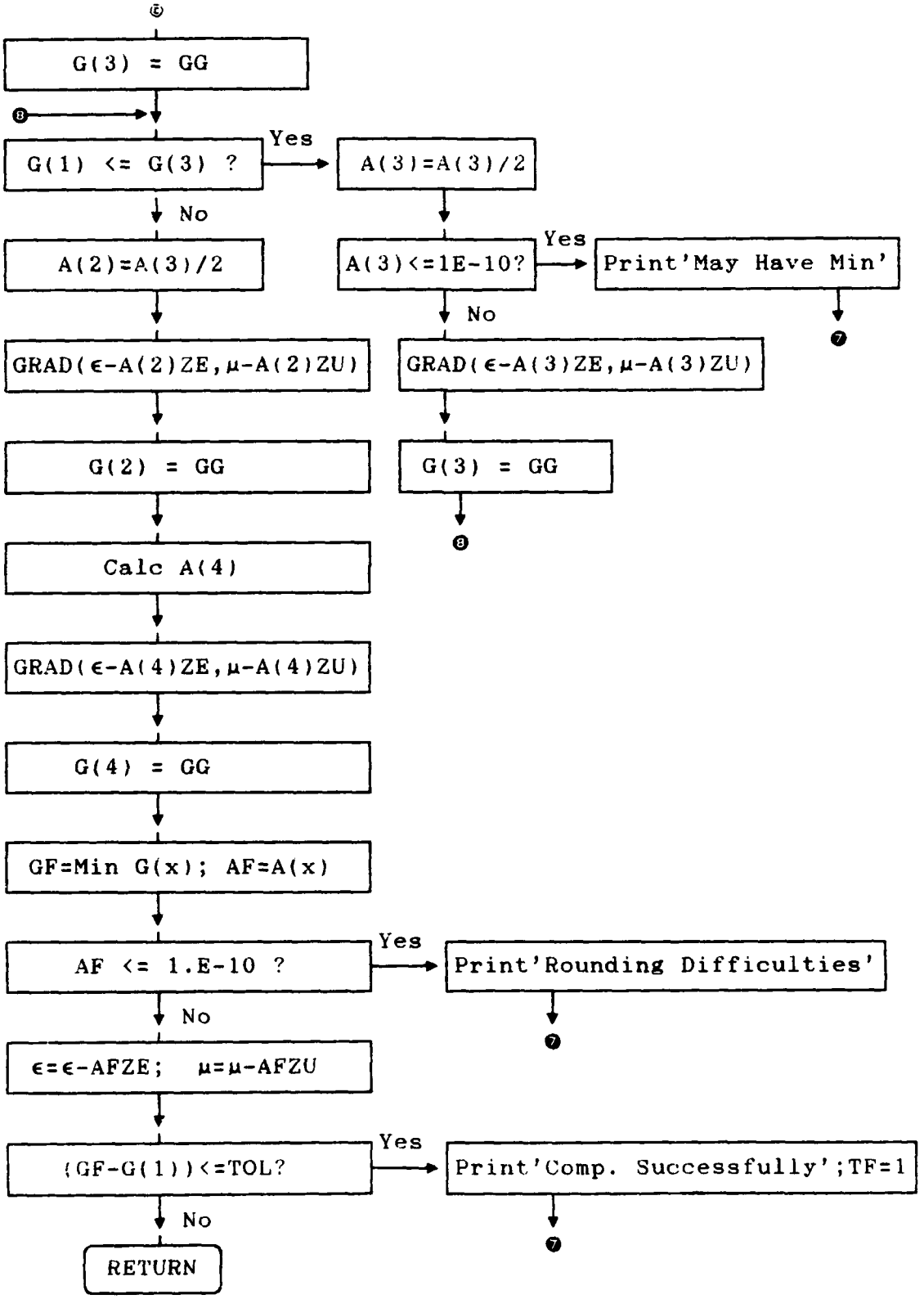
G(3) = GG
G(1) <= G(3) ?
Yes
A(3)=A(3)/2
No
A(2)=A(3)/2
A(3)<=1E-10?
Yes
Print'May Have Min'
No
GRAD(ϵ-A(2)ZE,μ-A(2)ZU)
GRAD(ϵ-A(3)ZE,μ-A(3)ZU)
G(2) = GG
G(3) = GG
Calc A(4)
GRAD(ϵ-A(4)ZE,μ-A(4)ZU)
G(4) = GG
GF=Min G(x); AF=A(x)
AF <= 1.E-10 ?
Yes
Print'Rounding Difficulties'
No
ϵ=ϵ-AFZE; μ=μ-AFZU
(GF-G(1))<=TOL?
Yes
Print'Comp. Successfully';TF=1
No
RETURN

Newton Algorithm

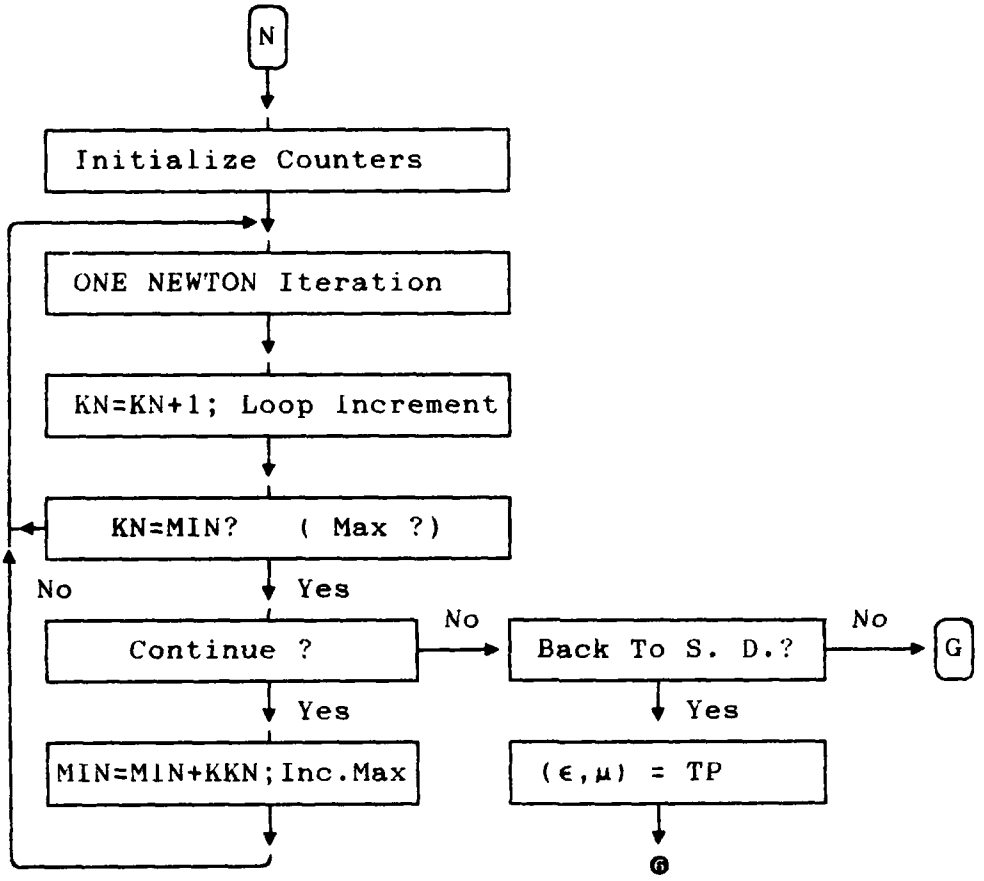

Restart

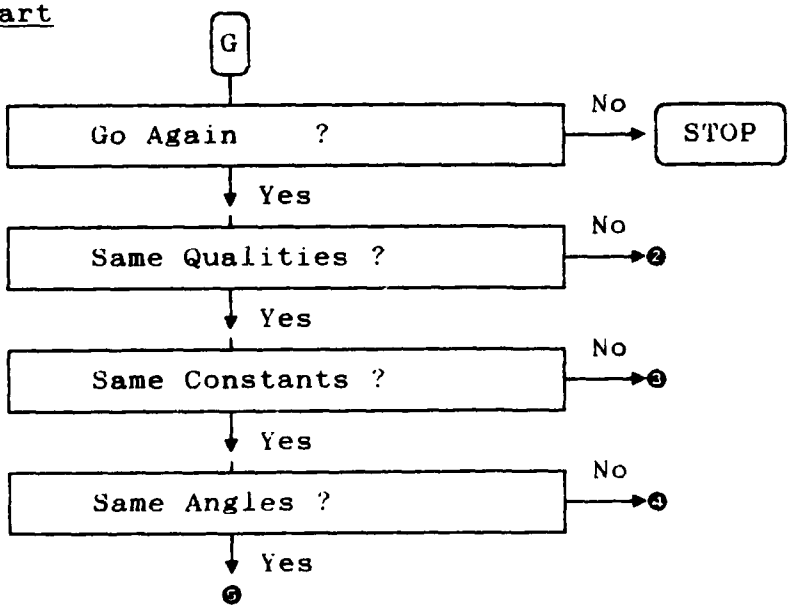

Listing

```
      PROGRAM MUEPS
      IMPLICIT DOUBLE PRECISION(A-G,P-Z)
      COMPLEX*16 E,U,ZE,ZU,CJ
      DIMENSION G(4),A(4),Y(4),X(4),TP(4)
      COMMON HH,AN(4,5),AR(4),TH(4),TA(4),TT(4),GG,W4,PL,DF,FL,FN
      COMMON ZE,ZU,CJ
C
C     INPUTS AND INITIALIZATIONS
C     Input Prior Quality Knowledge to Set System Order
C     Input Constants and Incidence Angle Set
C     Input Measured Transmission Magnitudes
C
  2   FN=1
      FL=1
      PRINT*,'MAGNETIC? (Y=1)'
      READ(5,*) QA
      PRINT*,' '
      IF(QA.NE.1) THEN
           FN=0
           X(3)=1
           X(4)=0
           PRINT*,'LOSSY? (Y=1)'
           READ(5,*) QA
           PRINT*,' '
           IF(QA.NE.1)THEN
                FL=0
                X(2)=0
           END IF
      END IF
  4   HH=(2)**(FN+FL)
C
  6   PRINT*,'INPUT F(GHZ), D(CM), POL. (perp=1,par1=0)'
      READ(5,*) FR,PT,PL
      IF(PL.NE.1)PL=0
      PRINT*,' '
      WRITE(6,13) FR
      WRITE(6,16) PT
      WRITE(6,17) PL
 13   FORMAT(1X,' FR = ',F7.4)
 16   FORMAT(1X,' PT = ',F7.4)
 17   FORMAT(1X,' PL = ',F7.4)
      PRINT*,' '
      WRITE(6,1)
      READ(5,*) QA
      IF(QA.NE.1)GO TO 6
C
 10   WRITE(6,11) HH
 11   FORMAT(1X,'INPUT',F3.0,' ANGLES')
      DO 15 JJ=1,HH
 15   READ(5,*) TH(JJ)
```

```
      PRINT*,' '
      PRINT*,'ANGLES ARE'
      DO 20 JJ=1,HH
20    WRITE(6,19) JJ,TH(JJ)
19    FORMAT(1X,'TH',I2,' = ',F5.2)
      PRINT*,' '
      WRITE(6,1)
      READ(5,*) QA
      PRINT*,' '
      IF(QA.NE.1)GO TO 10
C
22    PI=3.141592653589793238
      CJ=DCMPLX(0.0,1.0)
      W4=PI*PT*FR/29.97924574
      TOL=1.E-4
      TF=0
C
      PRINT*,'TEST? (Y=1)'
      READ(5,*) QT
      PRINT*,' '
      IF(QT.NE.1) QT=0
25    IF(QT.NE.1) THEN
            PRINT*,'INPUT INITIAL PARAMETER GUESSES'
            ELSE
            PRINT*,'INPUT SOLUTION PARAMETER VALUES'
      END IF
      DO 30 JJ=1,HH
30    READ(5,*) X(JJ)
      E=DCMPLX(X(1),-X(2))
      U=DCMPLX(X(3),-X(4))
      PRINT*,' '
      PRINT*,'ER = ',X(1),' EI = ',X(2)
      PRINT*,'UR = ',X(3),' UI = ',X(4)
      PRINT*,' '
      DF=0
      CALL GRAD(E,U)
      WRITE(6,14) TT
      IF(QT.EQ.1) THEN
            DO 35 JJ=1,HH
35          TA(JJ)=TT(JJ)
            PRINT*,' '
            WRITE(6,1)
            READ(5,*) QA
            PRINT*,' '
            IF(QA.NE.1) GO TO 25
            QT=2
            GO TO 25
      END IF
      PRINT*,' '
      WRITE(6,1)
      READ(5,*) QA
      PRINT*,' '
```

```
      IF(QA.NE.1) GO TO 25
      IF(QT.EQ.2) GO TO 53
C
40    PRINT*,'INPUT TRANSMISSION MEASUREMENTS'
      DO 45 JJ=1,HH
45    READ(5,*) TA(JJ)
      PRINT*,' '
      PRINT*,'TA = '
      DO 50 JJ=1,HH
50    PRINT*,TA(JJ)
      PRINT*,' '
      WRITE(6,1)
      READ(5,*) QA
      PRINT*,' '
      IF(QA.NE.1) GO TO 40
C
53    K=1
      KK=0
      MI=1
C
55    PRINT*,'GO DIRECTLY TO NEWTON? (Y=1)'
      READ(5,*) QA
      PRINT*,' '
      IF(QA.EQ.1) THEN
           DO 56 JJ=1,HH
56         TP(JJ)=X(JJ)
           GO TO 105
      END IF
C
C     STEEPEST DESCENT ALGORITHM
C     Each Iterative Loop Makes a Small Correction
C     to the Input Guess Parameter Set According
C     to the Steepest Descent Algorithm
C
58    DO WHILE(K.LE.MI)
      ZE=DCMPLX(0.0,0.0)
      ZU=DCMPLX(0.0,0.0)
      DF=1
      CALL GRAD(E,U)
      G(1)=GG
      Z0=CDABS(CDSQRT(ZE*DCONJG(ZE)+ZU*DCONJG(ZU)))
      IF(DABS(Z0).LT.1E-20) THEN
           WRITE(6,8)
           GO TO 100
      END IF
      ZE=ZE/Z0
      ZU=ZU/Z0
      A(1)=0.
      A(3)=1.
      DF=0
      CALL GRAD(E+A(3)*ZE,U+A(3)*ZU)
      G(3)=GG
```

```
      DO WHILE(G(1).LE.G(3))
           A(3)=A(3)/2.
           IF(A(3).LT.1.E-10) THEN
                WRITE(6,3)
                GO TO 100
           END IF
           CALL GRAD(E-A(3)*ZE,U-A(3)*ZU)
           G(3)=GG
      END DO
      A(2)=A(3)/2.
      CALL GRAD(E-A(2)*ZE,U-A(2)*ZU)
      G(2)=GG
      H1=(G(2)-G(1))/(A(2)-A(1))
      H2=(G(3)-G(2))/(A(3)-A(2))
      H3=(H2-H1)/(A(3)-A(1))
      A(4)=.5*(A(1)+A(2)-H1/H3)
      CALL GRAD(E-A(4)*ZE,U-A(4)*ZU)
      G(4)=GG
      GF=G(4)
      AF=A(4)
      DO 65 JJ=1,3
      IF(G(JJ).LT.GF) THEN
           GF=G(JJ)
           AF=A(JJ)
      END IF
65    CONTINUE
      IF(ABS(AF).LT.1.E-10) THEN
           WRITE(6,9)
           GO TO 100
      END IF
      E=E-AF*ZE
      U=U-AF*ZU
75    IF(ABS(GF-G(1)).LT.TOL) THEN
           WRITE(6,5)
           TF=1
           GO TO 100
      END IF
      K=K+1
      END DO
C
C     Iteration Loop Has Been Completed
C     Immediately Following are User Messages and Interactions
C
      WRITE(6,7)
      PRINT*,' '
      WRITE(6,12) K-1,DCONJG(E),DCONJG(U)
      PRINT*,' '
      DF=0
      CALL GRAD(E,U)
      WRITE(6,14) TT
      WRITE(6,24) TA
      PRINT*,' '
```

```
      PRINT*,'TOL=',ABS(GF-G(1))
      PRINT*,' '
      PRINT*,'CONTINUE? (YES=1)'
      READ(5,*) QA
      PRINT*,' '
      IF(QA.NE.1) GO TO 101
80    IF(TF.EQ.1) THEN
           PRINT*,'LOWER TOLERANCE (YES=1)'
           READ(5,*) QA
           PRINT*,' '
           IF(QA.NE.1) GO TO 120
           IF(QA.EQ.1) TOL=TOL*.1
           IF(QA.EQ.1) TF=0
           IF(QA.EQ.1) GO TO 75
      END IF
      PRINT*,'HOW MANY MORE ITERATIONS?'
      READ(5,*)KK
      PRINT*,' '
      MI=MI+KK
      GO TO 58
C
100   WRITE(6,12) K-1,DCONJG(E),DCONJG(U)
      PRINT*,' '
      DF=0
      CALL GRAD(E,U)
      WRITE(6,14) TT
      WRITE(6,24) TA
      PRINT*,' '
      PRINT*,'TOL=',ABS(GF-G(1))
      PRINT*,' '
C
101   PRINT*,'GO TO NEWTON (YES=1)'
      READ(5,*) QA
      PRINT*,' '
      IF(QA.EQ.1) THEN
           TP(1)=DREAL(E)
           TP(2)=-DIMAG(E)
           TP(3)=DREAL(U)
           TP(4)=-DIMAG(U)
           GO TO 105
      END IF
      IF(TF.EQ.1) GO TO 80
      GO TO 120
C
  1   FORMAT(1X,'ARE THESE VALUES CORRECT? (YES=1)')
 12   FORMAT(1X,I6,4F11.5)
 14   FORMAT(1X,' TT = ',4F11.5)
 24   FORMAT(1X,' TA = ',4F11.5)
  8   FORMAT(1X,'ZEROGRADIENT: MAY HAVE MIN')
  3   FORMAT(1X,'NO LIKELY IMPROVEMENT: MAY HAVE MIN')
  9   FORMAT(1X,'NO CHANGE LIKELY: PROBABLY ROUNDING DIFFICULTIES')
  5   FORMAT(1X,'PROCEEDURE COMPLETED SUCCESSFULLY')
```

```
 7    FORMAT(1X,'MAXIMUM ITERATIONS EXCEEDED')
C
C     NEWTON ALGORITHM
C     Each Iterative Loop Makes a Small Correction
C     to the Input Guess Parameter Set According
C     to the Newton Algorithm Method
C
105   KN=1
      MIN=1
110   DO WHILE(KN.LE.MIN)
      DF=1
      CALL GRAD(E,U)
      CALL GAUSS(Y)
      YM=DSQRT(Y(1)**2+Y(2)**2+Y(3)**2+Y(4)**2)
      IF(YM.LT.1.E-11) THEN
           WRITE(6,5)
           WRITE(6,12) KN,DCONJG(E),DCONJG(U)
           GO TO 111
      END IF
      E=E-Y(1)+Y(2)*CJ
      U=U-Y(3)+Y(4)*CJ
      KN=KN+1
      END DO
C
C     Iteration Loop Has Been Completed
C     Immediately Following are User Messages and Interactions
C
      WRITE(6,7)
      WRITE(6,12) KN-1,DCONJG(E),DCONJG(U)
      DF=0
      CALL GRAD(E,U)
      WRITE(6,14) TT
      WRITE(6,24) TA
      PRINT*,' '
      PRINT*,'CONTINUE? (YES=1)'
      READ(5,*) QA
      PRINT*,' '
      IF(QA.NE.1) GO TO 111
      PRINT*,'HOW MANY MORE ITERATIONS?'
      READ(5,*) KKN
      MIN=MIN+KKN
      GO TO 110
C
111   PRINT*,'GO BACK TO STEEPEST DESCENT? (YES=1)'
      READ(5,*) QA
      PRINT*,' '
      IF(QA.EQ.1) THEN
           E=DCMPLX(TP(1),-TP(2))
           U=DCMPLX(TP(3),-TP(4))
           GO TO 80
      END IF
C
```

```
C     Restart Routine
C     \llows Program to be Restarted to Run Again
C     with a Minimum of Repetitive Input from Previous Run
C
120   PRINT*,'GO AGAIN? (YES=1)'
      READ(5,*) QA
      PRINT*,' '
      IF(QA.NE.1) GO TO 150
      PRINT*,'WITH THE SAME QUALITIES? (YES=1)'
      PRINT*,' '
      IF(FN.EQ.1)THEN
           PRINT*,'MAGNETIC &'
           ELSE
           PRINT*,'NONMAGNETIC &'
      END IF
      IF(FL.EQ.1)THEN
           PRINT*,'LOSSY'
           ELSE
           PRINT*,'LOSSLESS'
      END IF
      PRINT*,' '
      READ(5,*) QA
      PRINT*,' '
      IF(QA.NE.1) GO TO 2
      PRINT*,'WITH THE SAME FREQ, D, POL (YES=1)'
      PRINT*,' '
      PRINT*,'FREQ = ',FR
      PRINT*,'   D = ',PT
      PRINT*,' POL = ',PL
      PRINT*,' '
      READ(5,*) QA
      PRINT*,' '
      IF(QA.NE.1) GO TO 6
      PRINT*,'WITH THE SAME ANGLES (YES=1)'
      PRINT*,' '
      DO 130 JJ=1,HH
130   WRITE(6,135) JJ,TH(JJ)
135   FORMAT(1X,'ANGLE',I3,' = ',F6.2)
      PRINT*,' '
      READ(5,*) QA
      PRINT*,' '
      IF(QA.NE.1) GO TO 10
      GO TO 22
150   STOP
      END
C
C     SUBROUTINE GRAD
C     Calculates Transmission Magnitudes, Error Functions
C     and Derivatives for Input Relative Parameter Values
C
      SUBROUTINE GRAD(CE,CU)
      IMPLICIT DOUBLE PRECISION(A-G,P-Z)
```

```
      COMPLX*16E,CU,ZE,ZU,CJ,I,D,ZZ,T,TM,W1,W2,W3,P1,P2,P3,BP1,BP2
      COMMON HH,AN(4,5),AR(4),TH(4),TA(4),TT(4),GG,W4,PL,DF,FL,FN
      COMMON ZE,ZU,CJ
C
      GG=0
      DO 200 O=1,HH
      I=CDSQRT(CE*CU-DSIND(TH(O))**2)
      D=2*W4*I
      ZZ=CU*DCOSD(TH(O))*PL/I+I*(1.-PL)/CE/DCOSD(TH(O))
      T=2/(2*CDOS(D)+CJ*(ZZ+1/ZZ)*CDSIN(D))
      TM=T*CONJG(T)
      TT(O)=-10.*DLOG10(CDABS(T))
      AR(O)=TT(O)-TA(O)
      GG=GG+AR(O)**2
      IF(DF.EQ.0) GO TO 200
      W1=W4/I
      W2=-DCOSD(TH(O))/2/I**3
      W3=1/(2*I*DCOSD(TH(O))*CE**2)
      P1=(2*CDSIN(D)-CJ*CDCOS(D)*(ZZ+1/ZZ))*W1*T
      P2=W2*PL*CU**2+(2*DSIND(TH(O))**2-CE*CU)*(1.-PL)*W3
      P3=W3*(1.-PL)*CE**2+(2*DSIND(TH(O))**2-CE*CU)*PL*W2
      BP1=P1*CU-CJ*CDSIN(D)*(1-1/ZZ**2)*T*P2
      BP2=P1*CE-CJ*CDSIN(D)*(1-1/ZZ**2)*T*P3
      AN(O,1)=-DREAL(BP1)
      AN(O,2)=-DIMAG(BP1)*FL
      AN(O,3)=-DREAL(BP2)*FN
      AN(O,4)=-DIMAG(BP2)*FN
180   ZE=ZE+AR(O)*(AN(O,1)-CJ*AN(O,2))
      ZU=ZU+AR(O)*(AN(O,3)-CJ*AN(O,4))
200   CONTINUE
      RETURN
      END
C
C     FUNCTION GAUSS
C     Solves Newton Method Matrix Equation
C     using Gaussian Elimination with Partial Pivoting
C
      FUNCTION GAUSS(Y)
      IMPLICIT DOUBLE PRECISION(A-G,P-Z)
      DIMENSION Y(4)
      COMMON HH,AN(4,5),AR(4)
C
      EE=2.718281828459045235
      DO 210 JJ=1,HH
210   AN(JJ,HH+1)=AR(JJ)/DLOG10(EE)/5.
      HM1=HH-1
      HP1=HH+1
      DO 280 I=1,HM1
      PVT=0
      DO 220 JJ=1,HH
      IF(PVT.GE.ABS(AN(JJ,I))) GO TO 220
      PVT=ABS(AN(JJ,I))
```

```
      IPVT=JJ
220   CONTINUE
      IF(PVT.EQ.0) GO TO 330
      IF(IPVT.EQ.I) GO TO 250
C
      DO 240 JJ=1,HP1
      TMP=AN(I,JJ)
      AN(I,JJ)=AN(IPVT,JJ)
      AN(IPVT,JJ)=TMP
240   CONTINUE
C
250   IP1=I+1
      DO 270 JJ=IP1,HH
      Q=-AN(JJ,I)/AN(I,I)
      AN(JJ,I)=0.
      DO 260 JK=IP1,HP1
      AN(JJ,JK)=Q*AN(I,JK)+AN(JJ,JK)
260   CONTINUE
270   CONTINUE
280   CONTINUE
      IF(AN(HH,HH).EQ.0) GO TO 330
C
      Y(HH)=AN(HH,HP1)/AN(HH,HH)
      DO 300 JJ=1,HM1
      Q=0
      DO 290 JK=1,JJ
      Q=Q+AN(HH-JJ,HP1-JK)*(Y(HP1-JK)
290   CONTINUE
      Y(HH-JJ)=(AN(HH-JJ,HP1)-Q)/AN(HH-JJ,HH-JJ)
300   CONTINUE
      RETURN
C
330   PRINT*,'ERROR'
      STOP
      END
```

Appendix C: Unaveraged Solution Data

AAP-ML-73 Solutions

Vertical Position and Angles		Horizontal Position (ϵ' | ϵ'')					
		Left		Center		Right	
Top	10-15	2.45560	1.27900	1.22988	0.99658	0.99600	0.84968
	10-20	1.95696	1.15400	1.21366	0.99085	0.88450	0.80738
	10-25	1.46869	1.01450	1.09570	0.94810	0.81896	0.78134
	15-20	1.46346	1.00896	1.20248	0.98666	0.81824	0.77901
	15-25	1.29812	0.95555	1.05970	0.93312	0.77585	0.76111
	20-25	1.19268	0.91699	0.96885	0.89414	0.74647	0.74699
Middle	10-15	1.08512	0.91270	1.03643	0.87568	1.11024	0.85836
	10-20	1.07790	0.91007	1.14070	0.91297	0.91089	0.78719
	10-25	1.08450	0.91250	1.04830	0.88000	0.86520	0.76987
	15-20	1.07290	0.90813	1.22430	0.94344	0.80425	0.74288
	15-25	1.08440	0.91243	1.05195	0.88150	0.80904	0.74483
	20-25	1.09323	0.91600	0.94675	0.83761	0.81263	0.74646
Bottom	10-15	1.82284	0.96718	1.18682	0.88019	1.43983	1.01778
	1(-20	1.49186	0.88248	1.15080	0.86825	1.06852	0.89284
	10-25	1.24712	0.81341	1.15799	0.87065	0.96414	0.85410
	15-20	1.31911	0.83183	1.12670	0.85966	0.89291	0.82206
	15-25	1.13460	0.77557	1.14954	0.86752	0.86973	0.81262
	20-25	1.02420	0.73637	1.16734	0.87410	0.85299	0.80503

Foiled AAP-ML-73 Solutions

Vertical Position and Angles		Horizontal Position (ϵ' | ϵ'')					
		Left		Center		Right	
Top	10-15	1.09594	0.88196	1.69636	1.14919	0.93419	0.82422
	10-20	1.51487	1.01779	1.17967	0.97982	0.76817	0.75834
	10-25	1.34332	0.96472	1.10482	0.95253	0.78256	0.76430
	15-20	2.02056	1.16505	0.95345	0.88934	0.67817	0.71657
	15-25	1.43818	0.99723	0.98994	0.90402	0.74500	0.74627
	20-25	1.16596	0.90044	1.01900	0.91655	0.80125	0.77310
Middle	10-15	1.44687	1.02686	0.96745	0.84272	1.22664	1.05032
	10-20	1.29335	0.97721	0.93106	0.82893	1.18162	1.03366
	10-25	1.26660	0.96827	0.92459	0.82645	1.10049	1.00289
	15-20	1.20110	0.94425	0.90704	0.81901	1.15151	1.02171
	15-25	1.21918	0.95060	0.91241	0.82115	1.06620	0.98814
	20-25	1.23326	0.95588	0.91647	0.82292	1.00779	0.96246
Bottom	10-15	1.54800	0.87783	1.09782	0.83946	0.97304	0.85347
	10-20	1.41612	0.84278	1.03725	0.81869	1.01055	0.86750
	10-25	1.27094	0.80220	1.00375	0.80695	0.87983	0.81749
	15-20	1.33529	0.81924	0.99831	0.80408	1.03807	0.87832
	15-25	1.20454	0.78076	0.97827	0.79675	0.85479	0.80616
	20-25	1.12060	0.75269	0.96367	0.79085	0.74878	0.75621

Half Hole AAP-ML-73 Solutions

Vertical Position and Angles		Horizontal Position (ϵ' | ϵ'')					
		Left		Center		Right	
Top	10-15	1.69082	1.07806	1.43418	1.06889	0.80464	0.77051
	10-20	1.52413	1.02909	1.16413	0.97602	0.69491	0.72453
	10-25	1.50894	1.02450	1.06442	0.93919	0.71304	0.73234
	15-20	1.42293	0.99654	1.02031	0.91912	0.63173	0.69396
	15-25	1.45991	1.00823	0.98217	0.90395	0.68915	0.72035
	20-25	1.48944	1.01806	0.95482	0.89191	0.73671	0.74402
Middle	10-15	1.00936	0.87450	0.68607	0.72909	0.76954	0.69104
	10-20	1.08554	0.90245	0.93125	0.82933	0.68529	0.65738
	10-25	1.07792	0.89969	0.94414	0.83424	0.74113	0.67988
	15-20	1.14443	0.92474	1.19226	0.92978	0.63560	0.63457
	15-25	1.10002	0.90856	1.05050	0.87857	0.73318	0.67620
	20-25	1.06826	0.89579	0.96097	0.84142	0.82123	0.71585
Bottom	10-15	1.26207	0.80278	1.42536	0.94614	0.74599	0.75983
	10-20	1.37316	0.83425	1.11217	0.84703	0.84767	0.80179
	10-25	1.18150	0.77907	0.96371	0.79528	0.85546	0.80490
	15-20	1.46230	0.85989	0.95637	0.78898	0.93081	0.83691
	15-25	1.15912	0.77158	0.87270	0.75717	0.89256	0.82159
	20-25	0.99826	0.71510	0.81785	0.73317	0.86548	0.80945

Whole Hole AAP-ML-73 Solutions

Vertical Position and Angles		Horizontal Position (ϵ' | ϵ'')					
		Left		Center		Right	
Top	10-15	1.18097	0.91948	1.03718	0.92815	0.57185	0.67096
	10-20	1.23794	0.93873	1.05590	0.93527	0.73450	0.74361
	10-25	1.29348	0.95708	1.03261	0.92641	0.75840	0.75366
	15-20	1.28072	0.95371	1.06931	0.94065	0.88833	0.81120
	15-25	1.33132	0.97057	1.03124	0.92583	0.82990	0.78731
	20-25	1.37236	0.98496	1.00385	0.91405	0.79011	0.76877
Middle	10-15	1.15388	0.92709	0.99760	0.85262	0.29759	0.47022
	10-20	1.05676	0.89234	0.87512	0.80595	0.35955	0.50495
	10-25	1.10308	0.90910	0.90519	0.81767	0.41590	0.53453
	15-20	0.99650	0.86854	0.80336	0.77495	0.40918	0.53498
	15-25	1.08849	0.90327	0.88029	0.80668	0.45869	0.56126
	20-25	1.16789	0.93451	0.94580	0.83528	0.49945	0.58555
Bottom	10-15	1.48391	0.86322	0.90826	0.77435	0.97624	0.85970
	10-20	1.22549	0.78936	0.88210	0.76458	1.02720	0.87875
	10-25	1.15985	0.76987	0.96330	0.79448	0.91250	0.83520
	15-20	1.23483	0.79226	0.86471	0.75749	1.06529	0.89362
	15-25	1.14493	0.76483	0.98070	0.80155	0.89476	0.82733
	20-25	1.08483	0.74417	1.08597	0.84291	0.79352	0.78077

Wet AAP-ML-73 Solutions

Vertical Position and Angles		Horizontal Position (ϵ' | ϵ'')					
		Left		Center		Right	
Middle	10-15	-------	-------	1.03619	0.87525	-------	-------
	10-20	-------	-------	1.07902	0.89077	-------	-------
	10-25	-------	-------	1.09657	0.89705	-------	-------
	15-20	-------	-------	1.11065	0.90277	-------	-------
	15-25	-------	-------	1.11587	0.90466	-------	-------
	20-25	-------	-------	1.11986	0.90622	-------	-------
Bottom	10-15	1.42271	0.84749	0.31631	1.19537	0.91642	0.83476
	10-20	1.44461	0.85343	0.99508	1.63235	1.05354	0.88636
	10-25	1.18115	0.77863	1.47503	1.87874	0.85802	0.81171
	15-20	1.46039	0.85790	2.23845	2.23442	1.16982	0.93033
	15-25	1.22660	0.75886	2.24969	2.33748	0.84179	0.80427
	20-25	0.95114	0.69731	2.73519	2.43116	0.68146	0.72641

Bibliography

1. Bertero, M. and others. "The Inverse Scattering Problem in the Born Approximation and the Number of Degrees of Freedom," Optics Acta, 27: 1011-1024 (1980).

2. Bolomey, J. C. and others. "Physically Motivated Approximations in some Inverse Scattering Problems," Radio Science, 17: 1567-1578 (November-December 1982).

3. Bolomey, J. C. and others. "Time Domain Integral Equation Applications for Inhomogeneous and Dispersive Slab Problems," IEEE TAP, 26: 658-667 (September 1978).

4. Borner, W-M. "Introduction to the Special Issue on Inverse Methods in Electromagnetics," IEEE TAP, 29: 185-89 (March 1981).

5. Bringi, V. N. and others. "Average Dielectric Properties of Discrete Random Media using Multiple Scattering Theory," IEEE TAP, 31: 371-375 (March 1983).

6. Burden, R. L. and J. D. Faires. Numerical Analysis. Boston: Prindle, Weber & Schmidt, 1985.

7. Colton, D. "The Inverse Electromagnetic Scattering Problem for a Perfectly Conducting Cylinder," IEEE TAP,29: 364-368 (March 1981).

8. Datta, A. K. and S. C. Som. "On the Inverse Scattering Problem for Dielectric Cylindrical Scatterers," IEEE TAP, 29: 392-397 (March 1981).

9. Johnson, L. W. and R. D. Riess. Numerical Analysis. Massachusetts: Addison-Wesley Publishing Company, 1982.

10. Joseph, J. C. Multiple Angle of Incidence Measurement Technigue for the Permittivity and Permeability of Lossy Materials at Millimeter Wavelengths. MS thesis, AFIT/GE/ENG/86D-58. School of Engineering, Air Force Institute of Technology (AU), Wright-Patterson AFB OH, December 1986.

11. Peterson, Andrew F. and Raj Mittra. "Convergence of the Conjugate Gradient Method when Applied to Matrix Equations Representing Electromagnetic Scattering Problems," IEEE TAP, 34: 1447-1454 (December 1986).

12. Roger, A. "Newton-Kantorovitch Algorithm Applied to an Electromagnetic Inverse Problem," IEEE TAP, 29: 232-238 (March 1981).

13. Shimabukuro, Fred I. and others. "A Quasi-Optical Method for Measuring the Complex Permittivity of Materials," IEEE TMTT, 32: 659-665 (July 1984).

14. Taylor, L. S. "Asymptotic Series Solution of the Paraxial Equation in Layered Media," IEEE TAP, 33: 1407-1410 (December 1985).

15. Tijhuis, A. G. "Iterative Determination of Permittivity and Conductivity Profiles of a Dielectric Slab in the Time Domain," IEEE TAP, 29: 239-245 (March 1981).

16. Wacker, P. F. "Uniform Theory of Near-Field Analysis and Measurement: Scattering and Inverse Scattering," IEEE TAP, 29: 342-351 (March 1981).

17. Weston, V. H. "Inverse Problem for the Reduced Wave Equation with Fixed Incident Field," Journal of Mathematical Physics, 21: 750-764 (1980).

VITA

Lieutenant Michael J. Walker [redacted] in 1983 and attended the United States Air Force Academy, from which he received the degree of Bachelor of Science in Electrical Engineering in May 1987. Upon graduation, he received a regular commission in the United States Air Force and entered the School of Engineering, Air Force Institute of Technology, in July 1987.

[redacted]

UNCLASSIFIED

SECURITY CLASSIFICATION OF THIS PAGE

REPORT DOCUMENTATION PAGE

Form Approved OMB No. 0704-0188

1a. REPORT SECURITY CLASSIFICATION UNCLASSIFIED	1b. RESTRICTIVE MARKINGS
2a. SECURITY CLASSIFICATION AUTHORITY	3. DISTRIBUTION/AVAILABILITY OF REPORT Approved for public release; distribution unlimited.
2b. DECLASSIFICATION/DOWNGRADING SCHEDULE	
4. PERFORMING ORGANIZATION REPORT NUMBER(S) AFIT/GE/ENG/88D-60	5. MONITORING ORGANIZATION REPORT NUMBER(S)
6a. NAME OF PERFORMING ORGANIZATION School of Engineering 6b. OFFICE SYMBOL (If applicable) AFIT/ENG	7a. NAME OF MONITORING ORGANIZATION
6c. ADDRESS (City, State, and ZIP Code) Air Force Institute of Technology Wright-Patterson AFB, OH 45433-6583	7b. ADDRESS (City, State, and ZIP Code)
8a. NAME OF FUNDING/SPONSORING ORGANIZATION AFWAL/AAWP-3 8b. OFFICE SYMBOL (If applicable)	9. PROCUREMENT INSTRUMENT IDENTIFICATION NUMBER
8c. ADDRESS (City, State, and ZIP Code) Wright-Patterson AFB, OH 45433	10. SOURCE OF FUNDING NUMBERS PROGRAM ELEMENT NO. / PROJECT NO. / TASK NO. / WORK UNIT ACCESSION NO.

11. TITLE (Include Security Classification)
A MICROWAVE MEASUREMENT TECHNIQUE FOR COMPLEX CONSTITUTIVE PARAMETERS

12. PERSONAL AUTHOR(S)
Michael J. Walker, B.S.E.E., 2Lt, USAF

13a. TYPE OF REPORT	13b. TIME COVERED	14. DATE OF REPORT (Year, Month, Day)	15. PAGE COUNT
MS Thesis	FROM _____ TO _____	1988 December	92

16. SUPPLEMENTARY NOTATION

17. COSATI CODES			18. SUBJECT TERMS (Continue on reverse if necessary and identify by block number)
FIELD	GROUP	SUB-GROUP	Radar Absorbing Materials, Millimeter Waves, Inhomogeneous Complex Parameter Measurement
14	02		
11			

19. ABSTRACT (Continue on reverse if necessary and identify by block number)

Thesis Chairman: Harry Barksdale, Major, USAF

Approved for public release IAW AFR 190-1
Distribution unlimited
12 Jan 1989

20. DISTRIBUTION/AVAILABILITY OF ABSTRACT	21. ABSTRACT SECURITY CLASSIFICATION
☒ UNCLASSIFIED/UNLIMITED ☐ SAME AS RPT. ☐ DTIC USERS	UNCLASSIFIED

22a. NAME OF RESPONSIBLE INDIVIDUAL	22b. TELEPHONE (Include Area Code)	22c. OFFICE SYMBOL
Harry Barksdale, Major, USAF	513-255-6027	AFIT/ENG

DD Form 1473, JUN 86 — Previous editions are obsolete. — SECURITY CLASSIFICATION OF THIS PAGE

UNCLASSIFIED

A technique was developed for the measurement of complex constitutive parameters of thin slabs of radiation absorbing material. Parameters include the real and imaginary components of the permittivity and permeability. The conductivity was lumped into a composite imaginary permittivity component through the loss tangent. The homogeneity of the material across the slab's surface and the ability of this technique to locate areas where the parameters deviate from the average was also examined.

The transmission coefficients of the slabs were measured at several angles of incidence using a 180 degree, bistatic configuration. This permitted a computer program to solve the nonlinear system of transmission equations for the desired parameter values. The technique and computer program are applicable to measurements taken at either perpendicular or parallel polarization, and takes advantage of prior known material qualities, nonmagnetic or lossless, to reduce the order of the system. Measurements were taken at 94 GHz using a Gunn phase-locked oscillator as a source. A pair of conical horn-lens antennas and a Scientific Atlanta 1783 Programmable microwave receiver were the primary pieces of equipment required.

Tests and measurements showed this system was an improvement over previous capabilities. Pseudo-parameter variations of ten percent or more, produced by physical alteration of specific regions of the material, were detected in the parameter outputs even when they were not detectable in the measurement values alone.